HHS Public Access

Author manuscript

J Comp Neurol. Author manuscript; available in PMC 2017 May 01.

Published in final edited form as:

J Comp Neurol. 2016 May 1; 524(7): 1494–1526. doi:10.1002/cne.23921.

Intracortical connections are altered after long-standing deprivation of dorsal column inputs in the hand region of area 3b in squirrel monkeys

Chia-Chi Liao, **Jamie L. Reed**, **Jon H. Kaas**, and **Hui-Xin Qi**

Department of Psychology, Vanderbilt University, Nashville, TN 37240, USA

Abstract

A complete unilateral lesion of the dorsal column somatosensory pathway in the upper cervical spinal cord deactivates neurons in the hand region in contralateral somatosensory cortex (areas 3b and 1). Over weeks to months of recovery, parts of the hand region become reactivated by touch on the hand or face. In order to determine if changes in cortical connections potentially contribute to this reactivation, we injected tracers into electrophysiologically identified locations in cortex of area 3b representing the reactivated hand and normally activated face in adult squirrel monkeys. Our results indicated that most of the expected connections of area 3b remained for partially reactivated area 3b, including the majority of intrinsic connections within area 3b; feedback connections from area 1, secondary somatosensory cortex (S2), parietal ventral area (PV) and other cortical areas; and thalamic inputs from the ventroposterior lateral nucleus (VPL). In addition, tracer injections in the reactivated hand region of area 3b labeled more neurons in the face and shoulder regions of area 3b than in normal monkeys, and injections in the face region of area 3b labeled more neurons in the hand region. Unexpectedly, the intrinsic connections within area 3b hand cortex were more widespread after incomplete dorsal column lesions (DCLs) than after a complete DCL. Although these additional connections were limited, these changes in connections may contribute to the reactivation process after injuries.

Graphic Abstract

*Corresponding author: Name: Hui-Xin Qi, Address: 301 Wilson Hall, Department of Psychology, Vanderbilt University, 111 21st Avenue South, Nashville, TN 37240, Phone: +1-615-322-5247, Fax: +1-615-343-8449, huixin.qi@vanderbilt.edu.

CONFLICT OF INTEREST STATEMENT: The authors have no conflict of interest.

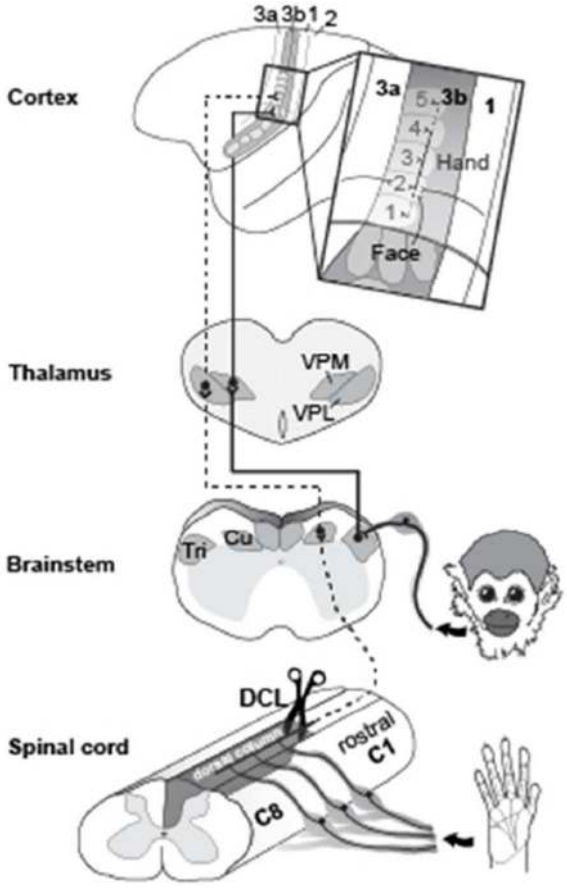

Authors used anatomical tracing method to reveal how intracortical connections of area 3b neurons contribute to the cortical reactivation in long-standing DCL monkeys. More widespread connections within area 3b and feedback projections from area 1 and other cortical areas to the reactivated hand region of area 3b are shown.

Keywords

cortical plasticity; somatosensory cortex; cuneate nucleus; ventroposterior nucleus; spinal cord injury; axon growth

INTRODUCTION

Interruptions of dorsal column inputs at the cervical spinal cord deprive neurons in the somatosensory system of their cutaneous inputs from the hand (Kaas et al., 2008; Qi et al., 2014a). Over weeks to months of recovery after dorsal column lesions (DCLs, see Table 1 for all abbreviations), some neurons in the hand region of primary somatosensory area 3b remain unresponsive and others become responsive to touch on adjacent parts of hand that are spared from the injury (Chen et al., 2012; Qi et al., 2011a; Qi et al., 2014b; Yang et al., 2014). However, in monkeys with longer recovery times of 8 months or more, there is evidence that inputs from other parts of the body such as face or forelimb intrude into the

deprived hand region in area 3b, resulting in a large-scale cortical reorganization (Jain et al., 1997; Jain et al., 2008; Kambi et al., 2014). Such abnormal representations in the deprived region in the somatosensory cortex have been attributed to rewiring of anatomical connections at subcortical stations such as the brainstem (Jain et al., 2000; Kambi et al., 2014) or thalamus (Li et al., 2014) in different sensory loss models. However, it is not known whether the organizations of the cortical and thalamic connections of area 3b neurons are altered after DCLs in ways that could contribute to the reorganized somatotopy in the hand region of somatosensory cortex (Fig. 1).

In the somatosensory system of monkeys, the forelimb, hand, and face regions in area 3b are somatotopically organized in a mediolateral sequence and can be approximately identified by physiologically and anatomically defined borders (Cerkevich et al., 2014; Fang et al., 2002; Jain et al., 1998; Merzenich et al., 1984; Qi and Kaas, 2004; Sur et al., 1982; Wall and Kaas, 1986). The hand region is anatomically identified at the mediolateral level of tip of the central sulcus, and the forelimb region is located medially. Laterally, the hand region is neighbored by the face region with an anatomically defined hand/face border. The representations of digits 1–5 are arranged in a lateromedial sequence in the rostral aspect and the representations of palm pads are arranged caudally in the anatomically defined hand region (Sur et al., 1982). Laterally in the face region, representations of lower lip, chin, upper lip, and upper face are arranged in an orderly rostrocaudal sequence. Although area 3b neurons normally have dense and extensive connections within area 3b and to other areas of somatosensory cortex including areas 3a, 1, 2, primary motor cortex (M1), and PV/S2, these intracortical connections are largely confined to regions that represent the same and/or adjoining body parts (Burton and Fabri, 1995; Fang et al., 2002; Liao et al., 2013; Manger et al., 1997; Negyessy et al., 2013). Rarely do the connections extend beyond the borders of the somatotopically matched regions. However, in monkeys with a long-standing loss of inputs from the hand, tracer injections in the deprived hand region of area 1 that became responsive to stimuli on face and forelimb showed markedly expanded distributions of labeled neurons into the face and forearm regions in areas 3b and 1 (Florence et al., 1998). This finding revealed the possibility that the intracortical connections of the somatosensory cortex could be anatomically altered after a long-standing sensory loss, possibly accounting for the formation of the abnormal somatotopic organization in the cortex that occurs over longer recovery times.

Here we test this possibility by studying the organization of intracortical connections of neurons in the reactivated hand region and the normal unaffected face region in area 3b after long-standing DCLs, and relate these connections to the altered somatotopic representations in cortex using functional maps in areas 3b and 1. We were particularly interested in connections of area 3b because it receives driving inputs from the ventroposterior thalamic nucleus (VP) and has dense reciprocal connections to other somatosensory cortical areas (Burton and Fabri, 1995; Jones and Friedman, 1982; Lin et al., 1979). We predicted that if intracortical connections of area 3b contribute to the cortical reactivation after DCLs, the pattern of anatomical connections and functional representations would be altered. Thus, we made unilateral DCLs at C4-C6 levels in four squirrel monkeys. When placed at the C4 level, this type of lesion disrupts the pathway for touch sensation from the hand and deprives the corresponding territory in contralateral area 3b of activating inputs. When placed at the

C5/C6 level, the unilateral DCL preserves some activating inputs from digit 1 or digits 1 and 2 (which enter the spinal cord above the C6 level). After 9–14 months of recovery to allow enough time for large-scale cortical reactivation to occur (Jain et al., 1997), microelectrode recordings were used to map the hand and face regions in areas 3b and 1 contralateral to the DCL. Cholera toxin subunit B (CTB) was injected into the reorganized hand region of area 3b. Biotinylated dextran amine (BDA) was injected into the face region of area 3b. The locations of labeled neurons were plotted and compared to the altered somatotopic representations in areas 3b and 1. This strategy allowed us to evaluate the connections of the hand and face injection site regions (Liao et al., 2013). Since plasticity at subcortical stations including the thalamus and brainstem is suggested to contribute to the cortical reactivations after injuries (Jain et al., 2000; Kambi et al., 2014; Li et al., 2014; Li et al., 2013), we also examined the connections of the hand and face regions in the thalamus and brainstem. Overall, the present study provides system-wide observations of connectional organization in the cortex, thalamus, and brainstem after long-standing DCLs. We demonstrate that the intracortical connections of the area 3b hand neurons are anatomically altered after long-standing DCLs by forming more widespread connections within area 3b and to other somatosensory cortex, especially in monkeys with incomplete DCLs. We speculate such altered intracortical connections of area 3b contribute to the cortical reactivation by integrating effective inputs from the periphery to area 3b and widespread projections from other areas of somatosensory cortex.

MATERIALS AND METHODS

We identified the organization of intracortical connections of the hand and face regions in area 3b after long-standing loss of primary afferents from the hand in four squirrel monkeys (2 *Saimiri boliviensis boliviensis*, 1 *Saimiri boliviensis peruviensis*, 1 *Saimiri sciureus*,). For comparisons, we used data collected from 2 normal squirrel monkeys in our previous study (Liao et al., 2013). Electrophysiological recordings were used to map the topographic organization in area 3b and neuroanatomical tracing methods were used to reveal the intrinsic connections and feedback connections of area 3b neurons. All surgical and animal care procedures were conducted in accordance with the Guide for the Care and Use of Laboratory Animals by the National Institutes of Health and approved by the Animal Care and Use Committee of Vanderbilt University.

Unilateral DCLs

To evaluate whether spared inputs from the hand affect the rewiring of intracortical connections of the deprived hand region in area 3b, we made DCLs at different levels in four monkeys. In monkey SM-J, we made a DCL at C4 on the right side to fully remove inputs from the hand and part of the forelimb. In monkey SM-Y, the dorsal column on the left side was cut at the C5/C6 level, which spared inputs from digit 1 and a portion of digit 2. In monkey SM-U, the dorsal column on the left side was cut at the rostral C5 level to remove inputs from digits 1–5. Monkey SM-T received two DCL surgeries on the left side. The first lesion was at rostral C5, whereas the second lesion was placed slightly rostral to the first lesion site at the C4/C5 level 44 days after the first lesion.

In preparation for the surgery, monkeys were initially tranquilized with an intramuscular injection of ketamine hydrochloride (10–25 mg/ kg) and anesthesia was continued by inhaled isoflurane (1–2% mixed in O_2). While fully anesthetized, monkeys were placed in a stereotaxic frame. Exposure of the cervical spinal cord was performed under aseptic conditions. Vital signs including heart rate, respiration rate, blood temperature, expiration CO_2, and arterial O_2 saturation were monitored every 10 min throughout the procedure. An incision was made in the skin at the midline over the cervical spinal cord. We retracted the muscles covering the cervical spinal cord, removed the dorsal arch of the vertebrae, and retracted dura and pia to expose the target region of the spinal cord. For the most complete lesion in monkey SM-J, we used fine forceps to clamp the dorsal column at cervical levels C3-C4 for two minutes, followed by a cut with a pair of iris surgical scissors at the same location. In the other 3 cases with incomplete lesions, the dorsal column was directly cut with a pair of iris surgical scissors. The dura was replaced by a piece of gel film, and then covered with gel foam. The incision site was then closed. Each monkey's recovery from anesthesia was closely monitored. Analgesics and antibiotics were given every 12 hours for 3 consecutive days.

Behavior training

The monkeys' performance on a reach-to-grasp task using the affected hand was tested 1–5 times per week (for details see Qi et al., 2013). The test was performed in the animals' home cages, which have two square apertures to provide access to the feeding tray. We replaced the feeding tray with a modified Kluver Board (15.2 cm × 9.9 cm) including 4 wells with various diameters (0.78 cm, 1.20 cm, 1.14 cm, and 1.14 cm) and depths (0.14 cm, 0.28 cm, 0.38 cm, and 0.64 cm) that represented incremental difficulties. For each trial, a 45 mg dustless precision banana-flavored pellet (product #F0021, Bioserve Inc., Frenchtown, NJ) was placed in the well directly in front of the aperture, which allowed monkeys to reach and retrieve the food pellet. The test was carried out in a randomized order between the 4 wells for 2 – 4 weeks pre-lesion, and starting from post-lesion week 2 up to one week before the final experiment.

Microelectrode recordings and tracer injections

We mapped the hand and face regions in areas 3b and 1 contralateral to the DCL side by microelectrode multiunit recordings over months of recovery (SM-J, 285 days; SM-Y, 292 days; SM-U, 414 days; SM-T, 321 days after the second DCL surgery). The main purpose of such electrophysiological mapping is to identify the responsive and unresponsive zones of the topographic maps in somatosensory cortex of each animal. An initial mapping session was used to determine the locations to inject tracers in area 3b. A later mapping session with dense microelectrode penetrations of responsive and unresponsive zones was used to reconstruct the regions containing labeled neurons and terminals for our estimates of connection densities. Monkeys were tranquilized with ketamine hydrochloride (10–25mg/kg, IM), and maintained anesthetized by an inhalation of isoflurane (1–2% in O_2), and placed in a stereotaxic head-holder. Vital signs were monitored throughout the procedures. Unilateral craniotomies were made over parietal cortex to expose the hand and face regions in area 3b.

Multiunit microelectrode mapping—The anesthesia was transitioned to an intravenous administration of ketamine hydrochloride (12 mg/kg/hr). Recordings were obtained with low-impedance tungsten microelectrodes (1 MΩ at 1KHz) that were lowered perpendicularly through the cortical surface to a depth of 650 μm where cortical layer 4 was located. We systematically placed the microelectrode every 500 μm to examine the evoked neuronal activities across regions of the hand and face in area 3b (Sur et al., 1982). The receptive fields of each penetration site were determined by standard mapping methods such as lightly touching and brushing the skin, tapping the muscles, and moving the joints (Qi et al., 2011a). The boundaries of area 3b with adjacent areas 1 and 3a were identified based on reversed somatotopies and distinguishable neuronal responses to peripheral stimulation (Sur et al., 1982). Neurons in area 3b have small, discrete receptive fields and are sensitive to low threshold, cutaneous stimulation. Area 3a neurons are distinguished by a tendency to respond to tapping and muscle or joint manipulations. Area 1 neurons respond to touch, but generally have larger receptive fields. Locations of each microelectrode penetration were marked on a photograph of the brain surface and the modalities and strengths of neuronal responsiveness were documented. Based on the well-established somatotopic maps in areas 3b and 1 in squirrel monkeys (Liao et al., 2013; Qi et al., 2011; Sur et al., 1982), we defined the 'hand region' in area 3b as the cortex that is medial to the anatomical hand/face border and lateral to the tip of central sulcus. The hand/face border is an anatomical landmark that does not change even after long-term sensory loss (Jain et al., 1998). The cortex lateral to the hand/face border is defined as the 'face region', and the cortex medial to the dimple of the central sulcus is defined as the 'forelimb region'. The lateromedial extents of the hand, face, and forelimb regions in area 3b were used to estimate these somatotopic regions in adjacent areas including areas 3a, 1, 2, and M1. In addition, we used 'representation' to define the territories in the cortex that were responsive to touch on hand, face, or forelimb during electrophysiological mapping. Thus, use of term 'region' in this context relates to anatomical territories, while 'representation' is associated with responses of multiunit activity.

Cortical tracer injections—Tracers were injected with 1-μl or 2-μl Hamilton syringes that had a glass pipette drawn to a fine tip attached. In each monkey, 0.05 μl of 1% CTB (Sigma, St. Louis, MO) in distilled water was injected into the hand region in area 3b. In most monkeys, this CTB injection was placed in the electrophysiologically defined digit 2 representation; however, when we could not identify responses to touch on digit 2 (SM-J) the injection was placed in the expected location of digit 2 (~1.5 mm from the hand/face border). We injected another tracer, BDA, in the face region of area 3b to reveal whether face neurons were connected to the hand cortex after DCLs. Specifically, 0.1 μl of 10% BDA (MW 10,000; Invitrogen, Carlsbad, CA) in pH 7.4 phosphate buffer was injected into the chin representation in area 3b (~1 mm lateral to the hand/face border). BDA is often used as a bidirectional tracer to label anterograde terminations and retrograde cell bodies (Imura and Rockland, 2007; Kultas-Ilinsky et al., 2003). For each injection site, tracer was first injected at a depth of 800 μm, and the second injection was placed at 600 μm. This strategy allowed the tracer to spread through supragranular layers, which have reciprocal connections to other cortical areas, and layer 4, which receives ascending projections from the thalamus (Felleman and Van Essen, 1991). Micropipettes were kept in position for 2 and

5 minutes after each injection to minimize tracer backflow. After the syringes were withdrawn, the dura was replaced by a piece of Gelfilm. The opening in the skull was covered with dental cement. Monkeys were monitored closely as they recovered from anesthesia, and analgesics and prophylactic antibiotics were given every 12 hours for 3 consecutive days.

Subcutaneous digit and chin tracer injections

As a measure of the completeness of the DCLs, CTB was subcutaneously injected into distal parts of glabrous digits 1, 3, and 5 of both hands and transganglionic transport through the nerves labeled terminals in the cuneate nucleus of the brainstem. The results allowed us to quantify and compare the areas of the labeled axon terminal fields in the left and right cuneate nuclei, which received intact or interrupted dorsal column inputs (Qi et al., 2011a). To determine if primary inputs from the face expand into the cuneate nucleus (Cu) after long-term recovery from DCLs, we injected another tracer, cholera toxin subunit B conjugated with wheat germ agglutinin-horseradish peroxidase (B-HRP, 0.2% in distilled water, List Biological, Campbell, CA), into the skin of the anterior chin ipsilateral to the side of the DCL. To allow sufficient tracer transport time, CTB and B-HRP tracers were placed 5 days before the terminal mapping procedure. In preparation for the injections, each monkey was tranquilized with ketamine hydrochloride (10–25 mg/kg, IM), and transitioned to inhaled isoflurane (1–2% in O_2). While anesthesia was at a surgical level, subcutaneous injections were made with Hamilton syringes to deliver 5 μl of tracer solution in the hands or chin (CTB or B-HRP, respectively), and monkeys were monitored during recovery from anesthesia.

Terminal microelectrode multiunit recordings

Two to three weeks after cortical tracer injections, microelectrode multiunit recordings were used to map representations of the hand and face in areas 3b and 1. Procedures were similar to the microelectrode recordings used in the aseptic survival surgery, but the distance between microelectrode recording sites was decreased from every 500 to about every 300 μm to obtain detailed maps of the hand and face regions. Special care was taken to identify rostral and caudal borders of areas 3b and 1, which were marked by small electrolytic lesions that were later identified histologically. Locations of microelectrode penetrations and lesion sites were marked on the printed image of the brain surface for later alignment of plots of labeled neurons.

Perfusion and histology

At the conclusion of mapping, monkeys were deeply anesthetized by a lethal dose of sodium pentobarbital (120 mg/kg, intravenously). When areflexive, the animal was perfused transcardially with phosphate buffered saline (pH 7.4), followed by 2% paraformaldehyde in phosphate buffer and 10% sucrose containing fixative. Brains were extracted from the skull and cortical hemispheres were carefully separated from the subcortical tissue, manually flattened, and post-fixed in 30% sucrose solution containing fixative at 4°C overnight. The subcortical tissue containing thalamus, brainstem, and cervical spinal cord were also extracted and kept in 30% sucrose solution containing phosphate buffer at 4°C overnight. Cervical segments were identified based on rostrocaudally arranged dorsal roots and by

placements of pins dorsoventrally through the spinal cord to mark selected segments. We cut cortical hemispheres in parallel to the cortical surface at a 40 μm thickness to facilitate the superimposing of the plotting results on the topographic maps identified by electrophysiological mapping in areas 3b and 1. The thalamus was cut in the coronal plane at 50 μm and brainstem was cut in a transverse plane at 40–60 μm. The spinal cord was cut in a horizontal plane at 40 μm. Sections were saved in series for different histological processes.

We processed the sections of cortex and thalamus in two stages to visualize labeling from CTB and BDA injections (see details in Liao et al., 2013). In brief, sections were first processed with a standard ABC- 3,3-diaminobenzidine tetrahydrochloride (DAB)-H_2O_2 reaction to reveal BDA-labeled neurons and axonal terminals with a brown reaction product. The staining was continued in the same sections to reveal the CTB label by immersing the sections in the primary antibody solution (goat anti-CTB, List Biological Labs) for 4 nights at 4°C. After repeated rinses, sections were incubated in the secondary antibody solution for one hour (PK-4005; Vector Laboratories, Burlingame, CA) and in the ABC solution for one hour. Finally, sections were reacted in the VIP substrate solution (SK-4600; Vector Laboratories) to show CTB-labeled neurons with a pink reaction product. One separate series of cortical sections was only processed to reveal BDA staining. In the third series, myelin fiber staining was used to reveal the areal borders of cortical regions and the hand/face borders in areas 3b and 1 (Cerkevich et al., 2014; Jain et al., 1998; Jain et al., 2001). One series of brainstem sections was processed for WGA-HRP staining by a standard method 3,3,5,5-tetramethylbenzidine reaction (TMB; Gibson et al., 1984) to reveal the projections from the skin of the anterior chin. Another series of brainstem and spinal cord sections were processed for CTB staining to reveal label from tracer injections in digits 1, 3, and 5 of both hands. We used cytochrome oxidase (CO; Wong-Riley 1979) and VGLUT2 staining (Liao et al., 2014; Qi et al., 2011b) in separate series to reveal architecture in the thalamus, brainstem, and spinal cord.

Antibody characterization

VGLUT2 antibodies were used in the present study (VGLUT2: AB_2187552; Table 2). Monoclonal anti-VGLUT2 (MAB5504, Millipore, Billerica, MA) is a mouse IgG1 antibody with clone 8G9.2, which was developed against the full length of recombinant protein from rat VGLUT2, and labels a single band at 56kDa (Balaram et al., 2013). Immunoreactivity of anti-VGLUT2 accurately recognizes VGLUT2 in primates (Balaram et al., 2013; Balaram and Kaas, 2014; Baldwin et al., 2013; Liao et al., 2015) and rats (Kaneko and Fujiyama, 2002).

Data analysis

Evaluation of the level and extent of DCL—CTB injections in digits 1, 3, and 5 labeled primary afferents near the cervical levels of C5, C6, and C7 in the spinal cord (Florence et al., 1989, 1991; Qi et al., 2011a). Observations of CTB-labeled patches in the horizontal plane allowed us to determine the level of the DCL in the spinal cord. We used two methods to evaluate the completeness of DCLs. First, a transverse view of the lesion site was reconstructed from a series of horizontal sections of the spinal cord in Adobe Illustrator

(Adobe Systems, San Jose, CA). In brief, images of spinal cord sections were digitally captured in a dorsal to ventral sequence. We aligned the images of sections using landmarks along the midline and pinholes. Then, to produce a transverse view of the lesion site, we measured the maximal extents of the lesion, the white matter, and the gray matter across every section. Second, CTB injected into matching locations of both hands labeled primary afferents from the hands on the lesioned side and intact side of the brainstem. We measured areas and optical intensities of CTB-labeled regions in the brainstem cuneate nuclei on the two sides using ImageJ 64 software (National Institutes of Health, Bethesda, MD). The areas and optical intensities of CTB-labeled regions on the two sides across the brainstem sections were statistically compared using the signed-rank test (SigmaPlot 11.0, San Jose, CA, see Liao et al., 2014). Statistical significance was considered for $p < 0.05$. The ratio of CTB-labeled axonal regions in the Cu on the lesioned side compared to those on the intact side is used as a quantitative measure of the surviving inputs from the hand after the DCL (see details in Qi et al., 2011).

Reconstruction of somatotopic map in the cortex—Based on the receptive fields and neuronal responsiveness defined by electrophysiological recordings, the representations of hand and face in areas 3b and 1 were reconstructed in Adobe Illustrator CS6. We scanned and imported the printed photograph of the exposed brain surface that was marked with locations of microelectrode penetrations into the Adobe Illustrator and reconstructed the map accordingly.

Determining the distributions of CTB- and BDA-labeled neurons and terminal fields—We systematically plotted the locations of CTB- and BDA-labeled neurons and terminals by using a Neurolucida system (MBF Bioscience, Williston, VT) that is attached to a Leica microscope (Aristoplan). Cortical sections processed with both CTB and BDA reactions were used to identify the CTB-labeled neurons, BDA-labeled neurons, and BDA-labeled terminals. Additionally, another set of cortical sections only processed with the BDA reaction was used to identify the BDA-labeled terminals. Special care was taken to mark tracer injection sites, blood vessels, landmarks, and electrolytic lesion sites for alignment of plotted label to adjacent fiber sections to define the areal borders and hand/face border in Adobe Illustrator. To evaluate connection densities of reactivated representations to the tracer injection sites, we superimposed the plots of CTB-labeled neurons, BDA-labeled neurons, and BDA-labeled terminals on the topographic maps in areas 3b and 1 that were identified by electrophysiological mapping. We counted the total number of CTB- and BDA-labeled neurons in the hand, forelimb, and face regions of areas 3b and 1 (see Liao et al., 2013). Our analysis mainly focused on the number of labeled neurons in each reactivated representation in the hand region of areas 3b and 1. Accordingly, the numbers of labeled neurons overlapping the territories that were responsive to touch on digits 1–5, palm, multiple digits and mixed receptive fields involving hand, face, or forelimb were categorized. Neurons overlapping the newly formed representations of forelimb and chin in the hand region were classified as ‘new forelimb’ and ‘new face’. Labeled neurons overlapping the territory that remained unresponsive to touch on hand, face and forelimb in the hand region were classified ‘Hand, NR’. The connectional densities of each somatotopic representation were converted to percentages by: 100 × the number of CTB- or BDA-

labeled neurons in each representation/ the total number of CTB- or BDA-labeled neurons in area 3b or 1. Also, the pattern of thalamocortical projections to area 3b after DCLs was analyzed by plotting the CTB- and BDA-labeled neurons and terminals from cortical injections in the VP. The plots were aligned to adjacent CO sections that revealed the structural architecture.

An upright brightfield/darkfield microscope (Nikon E800) was used to examine CTB- and BDA-labeled neurons and terminals in the cortex, CTB-labeled axonal terminals in the brainstem and spinal cord, and B-HRP-labeled axonal terminals in the brainstem. Images were digitally photographed with a Nikon DXM 1200 camera mounted on the microscope and exported to Adobe Photoshop CS6 (Adobe Systems) for adjustments of brightness and contrast.

Analysis of the distributions of CTB- and BDA- labeled neurons in cortex— Statistical methods were applied to analyze intracortical connections and how the proportions and locations of labeled neurons may be affected by the extent of the lesion in the spinal cord. Neuron counts and other case identifiers were listed in Excel and imported into IBM SPSS software (version 22, IBM, Armonk, NY) for statistical analyses. For all statistics, the significance level was set at 0.05 with two-tailed p values. First, one-sample Kolmogorov-Smirnov tests were used to compare the measures of labeled neurons (counts, percentages by cortical region, and total neurons per cortical area) to known families of distributions (normal, exponential, and uniform). The Kolmogorov-Smirnov tests indicated that measures of labeled neurons differed from the normal distribution ($p < 0.0001$); therefore, we used methods of generalized linear mixed modeling that are robust to violations of the assumptions of normal distributions and equal variances. Generalized linear models and generalized linear mixed models were used to model the data and estimate how the percentages of labeled neurons in regions of cortex may vary based on the lesion extent. Models selected were based on the normal distribution using the identity link function. We used a factor variable termed ‘DCL’ to indicate the lesion extent for each case (including 2 cases with no lesion) and a variable termed ‘Area’ to distinguish area 3b and area 1 within each case. Then within each Area, the percentages of labeled neurons were divided into categories for a factor variable termed ‘Response’ based on the electrophysiological mapping that provided estimated territories (~300 um map spacing) that were unresponsive to touch on the body (NR) or that responded to touch on the forelimb, face, and/or hand. Information including the DCL extent (0–100%); the injection site (area 3b hand or face region); the counts of labeled neurons in areas 3b and 1; the proportion of neurons (from counts of labeled neurons in areas 3b and 1) labeled in cortical regions (hand, face, forelimb, etc.) and subregions (digit 1, 2, etc.) that were estimated based on mapping and anatomical landmarks; Additionally, we used variables to identify the expected somatotopic region and neural responsiveness near the sites of the labeled neurons, and we combined this information into a variable termed, ‘Response’. For statistics, the Response variable includes broad zones for hand, forelimb, face, etc. For figures, the detailed responsive zones provide a more complete illustration of the results. We analyzed the main effects and interactions of DCL, Area, and Response to determine how these factors contributed to the differences in the percent of labeled neurons by regions. Differences in the tracer uptake may lead to

apparent differences between the numbers and locations of labeled neurons. Thus, the results from CTB injection in 3b hand and BDA injection in 3b face were analyzed separately. The sequential Bonferroni adjustment was applied for pair-wise comparisons. Additional details about the statistical methods are presented with the related results.

RESULTS

Our primary objective was to identify the organization of intracortical connections of affected hand neurons and (presumed unaffected) face neurons in area 3b after long-standing DCLs. We focused analyses on revealing functionalities of altered somatotopic representations, especially in the hand region in areas 3b and 1, in relation to the densities of anatomical connections to the tracer injection sites in area 3b after long-term injuries. Here, we first describe the level and extent of DCLs in each monkey, and how the DCLs resulted in alterations of somatotopy in areas 3b and 1. We then show the distributions of labeled neurons in the cortex after CTB was injected into the hand region of area 3b and BDA was injected into the face region of area 3b. Distributions of CTB- and BDA-label were plotted and compared to somatotopic maps in areas 3b and 1. To reveal whether DCLs resulted in alteration of connection patterns in the thalamus (Li et al., 2014) and brainstem (Jain et al., 2000; Kambi et al., 2014; Li et al., 2013), we examined how CTB and BDA injections in area 3b labeled neurons in the VP and how B-HRP injections in the skin of the anterior chin labeled axonal terminals in the brainstem. In each subsection, we describe results from four monkeys in an order based on the severity of DCLs.

Level and extents of DCLs

The level and severity of DCL differed in the four monkeys we studied (Figs. 2, 3). We identified the DCL extents using two approaches. First, a transverse view of DCL was reconstructed from series of horizontal spinal cord sections to show how the lesion site involved in the spinal cord. Second, we compared areas and optical densities of CTB-labeled terminals in the cuneate nuclei on the lesioned and intact sides throughout the brainstem sections to produce estimates of DCL completeness in each monkey (Qi et al., 2011a).

SM-J (100% DCL)—A complete DCL was made at the C4 level in monkey SM-J (Fig. 2A). The lesion site was restricted to the left side of the spinal cord and encroached into the entire cuneate fasciculus and spinal gray matter (Fig. 2A, left column). We confirmed the completeness of the lesion by injecting CTB into digits 1, 3, and 5 of both hands to label afferent projections from the lesioned and intact sides of the spinal cord (see Materials and Methods). On the intact side, there were three CTB-labeled patches along the medial region of spinal cord (Fig. 2A, middle column). The projections continued to ascend to the Cu and there were three labeled patches that corresponded to digits 1, 3, and 5 territories in a ventral to dorsal sequence (Fig. 2A, arrowheads in the right column). The combined area of labeled terminals across brainstem sections was 0.7 mm^2 (Fig. 3A). Although three CTB-labeled patches were present in the matching locations of the spinal cord on the left (lesioned) side, no CTB-labeled axonal terminals were shown in the left Cu in the brainstem, suggesting that the pathway was completely interrupted by the DCL. Accordingly, we estimated that all primary afferents from the left hand were cut in monkey SM-J.

SM-U (86% DCL)—We made a DCL in monkey SM-U at rostral C5 to cut inputs from digits 1–5 (Fig. 2B). The lesion was confined to the left side of spinal cord, extending into the cuneate fasciculus, dorsal horn, intermediate zone, and medial portion of the ventral horn. The most medial region of the dorsal column, the gracile fasciculus, was avoided. CTB injections into both hands labeled three dense patches near C5, C6, and C7 on both sides of the spinal cord. Three labeled patches in the Cu on the right side confirmed the intact projection from the right hand. Three CTB-labeled patches were found in the matching locations in the left Cu, but with much smaller areas. Areal measurement of CTB-labeled regions across rostrocaudal sections indicated that the combined area of labeled regions was 0.04 mm^2 on the left (lesioned) side and 0.3 mm^2 on the right (intact) side ($p < 0.001$), producing an estimation of an 86% reduction of inputs from the left hand (Fig. 3B, left column). No difference was detected in optical densities of labeled terminals in the cuneate nuclei on the two sides (Fig. 3B, right column).

SM-Y (65% DCL)—In monkey SM-Y, a DCL was made at the C5/C6 level of the right spinal cord, which was expected to interrupt inputs from a portion of digit 2, digits 3–5, and the connecting palm areas, but spare inputs from digit 1 and the ulnar portion of digit 2 (Fig. 2C). This lesion involved nearly the entire cuneate fasciculus, dorsal horn, intermediate zone, and ventral horn of the right spinal cord. The most ventrolateral region of the ventral horn was avoided. As expected, a dense CTB-labeled patch was found in the ventral aspect of Cu on the left side, corresponding to the digit 1 territory. We also noted weak CTB label in the expected location of digit 3, indicating that primary inputs from other digits were sparsely spared. Areal measurements of CTB-labeled regions in the cuneate nuclei on the left side (1.0 mm^2 in total; Fig. 3C) and on the right side (0.4 mm^2 in total) led to an estimate of a 65% complete DCL. The optical densities of labeled terminals in the cuneate nuclei on the two sides remained similar. Thus, the results indicated that peripheral inputs from digit 1, a portion of digit 2, and the radial palm were spared, but those from the ulnar side of digit 2, digits 3–5, and ulnar palm were mostly removed in this case.

SM-T (61% DCL)—Two DCL surgeries were performed in monkey SM-T to produce a deficit in reaching behavior. The first lesion (Fig. 2D, black shading in the left column) was made at the rostral C5 level, and the second one (Fig. 2D, dark gray shading in the left column) was made slightly rostral to the first lesion site at the C4/C5 level. Although the second lesion was more extensive, both lesions encroached into the cuneate fasciculus, dorsal horn, intermediate zone, and medial region of the ventral horn of the left spinal cord. The medial region of the intermediate zone of the right spinal gray matter was also involved. Combined areas of CTB-labeled regions across rostrocaudal brainstem sections (Fig. 3D; 0.3 mm^2 on the right side and 0.1 mm^2 on the left side) suggested that this DCL interrupted ~61% of projections from the digits 1–5 of the left hand.

Topographic maps in areas 3b and 1 after DCLs

We identified topographic maps of the hand and face regions in area 3b and the hand region in area 1 from these four monkeys with long recovery times after DCLs. As previously described by Sur et al. (1982), we found that the hand and face regions in area 3b were normally organized in a somatotopic manner (Liao et al., 2013). Representations of digits 1–

5 were arranged in an orderly lateral to medial sequence in the rostral aspect of area 3b, with the representation of the palm located caudally. The face region was located lateral to the hand region, with representations of lower lip, chin, and upper lip in a rostral to caudal sequence. The hand region in area 1 adjoined the hand region in area 3b caudally with the expected reversed somatotopic organization. In our DCL monkeys, differences in lesion level and extents resulted in various extents of cortical reactivation in the hand regions of areas 3b and 1 after 9–14 months of recovery, as reflected by large- to small-scale reorganization of somatotopic maps in the hand regions of areas 3b and 1.

SM-J (100% DCL)—We mapped the hand and face regions in area 3b contralateral to the DCL 285 days after a complete DCL in monkey SM-J (Fig. 4A). Complete deprival of tactile inputs from the contralateral hand caused a large-scale reorganization in the hand region of areas 3b and 1. Neurons in nearly half of the territory of the hand region in area 3b remained unresponsive to touch on the hand, face, and forelimb. However, when responsive, neuronal receptive fields were usually large and locations were abnormal. We did not find neurons responsive to touch on single glabrous digits 1–5 or palm pads, although neurons in patches of cortex responded to tapping on the hand. Instead, we found small populations of reactivated neurons in the hand territory that were responsive to touch on face or forelimb. Other reactivated hand neurons tended to have complex receptive fields involving forelimb and hand, face and hand, or forelimb and face, which has not been reported in area 3b in normal monkeys. Laterally in the face region of area 3b, neurons responsive to touch on the lower lip, chin, and upper lip were identified in an orderly rostral to caudal sequence, as in normal monkeys (Sur et al., 1982). Throughout the hand region in area 1, electrophysiological recordings found no neurons responsive to touch on hand, face, and forelimb. Our results revealed that the somatotopic maps in the hand region of areas 3b and 1 were entirely altered after the complete long-standing DCL. The somatotopic representations of the face in area 3b remained normal after injuries.

SM-U (86% DCL)—A reactivated but largely reorganized somatotopy was present in the hand regions of areas 3b and 1 after 414 days of recovery in monkey SM-U (Fig. 4B). We identified neurons responsive to touch on digits 2 and 4 in the expected locations of area 3b. One electrode penetration recorded neurons in the lateral region that responded to touch on digit 1. The representation of the palm was found in the caudolateral aspect of the hand region. Neurons in nearly half of the hand region in area 3b had large receptive fields involving multiple digits and the dorsal hand. Throughout the hand region in area 3b, we also found discontinuous distributions of neurons with complex receptive fields that were responsive to touch on the hand and forelimb. In the face region of area 3b, neurons responsive to touch on the lower lip, chin, and upper lip were arranged in normal somatotopic order, although neurons responsive to touch on the dorsal hand were found in a small territory lateral to the hand/face border. A somatotopically reversed map was identified in the hand region of area 1, although we encountered fewer reactivated neurons that had receptive fields involving the forelimb and hand. Representations of digit 4 and the palm were found in the expected locations in the lateral aspect of area 1, while other reactivated cortex mostly represented multiple digits and the dorsal hand.

SM-Y (65% DCL)—The hand and face regions in area 3b and the hand region in area 1 were mapped 292 days after the DCL in monkey SM-Y (Fig. 4C). Neurons responsive to touch on digits 1–4 were identified in the rostral aspect of the hand region in area 3b in normal somatotopic order from lateral to medial. However, the territories of digits 1 and 2 were enlarged and expanded medially. Additionally, patchy representations of digits 1 and 2 were present in unexpected locations in the hand region. The representation of digit 4 extended caudally into area 1. Neurons in approximately half of the territories with receptive fields in digits responded to touch on the dorsal and hairy part of digits. The representation of the palm was in the laterocaudal region adjacent to representations of digits 1 and 2, while the expected palm cortex in the medial region remained unresponsive. In the face region of area 3b, representations of the lower lip, chin, and upper lip were rostrocaudally identified. Again, a reversed but less reactivated hand map was found in the hand region in area 1. The representations of digits 1–4 were arranged lateromedially in the hand region in a discontinuous pattern, with the representation of the palm located in the laterorostral aspect of the area 1 hand region. Unexpectedly, we identified two territories medially in the hand region that were responsive to touch on digit 1 (which is normally represented laterally). Neurons in approximately half of the hand region in area 1 were mostly unresponsive to touch on hand, face, and forelimb.

SM-T (61% DCL)—Nearly normal somatotopy was identified in area 3b 321 days after the second DCL surgery in monkey SM-T (Fig. 4D). The representations of digits 1–5 were arranged lateromedially in the rostral aspect of the hand region of area 3b, with the representation of the palm caudally adjoining area 1. Few reactivated hand neurons had receptive fields involving multiple digits. The representations of lower lip, chin, and upper lip were identified in a normal order in the face region of area 3b. However, we found few neurons in the hand region of area 1 that were responsive after recovery. Neurons in small areas of the caudal hand region responded to touch on the glabrous and dorsal digits.

Distributions of neurons projecting to area 3b after DCLs

To reveal the patterns of intrinsic and feedback intracortical connections of the hand and face regions in area 3b after long-standing DCLs, we injected two different tracers in area 3b.. Although area 3b neurons are normally somatotopically connected within area 3b and to other cortical areas, Manger et al. (1997) reported that in macaque monkeys, neurons representing the lower jaw/neck in area 3b are located anatomically at the hand/face border and normally have intracortical connections with the hand region, particularly the digit 1 representation. Here we purposely targeted tracer injection sites beyond that border region to reveal any large-scale sprouting across the border between the hand and face regions. CTB was injected into the hand region, primarily the expected location of digit 2, and BDA was injected into the chin representation in face region after electrophysiological recordings. Distributions of CTB- and BDA-label were plotted on the flattened cortex parallel to the cortical surface, which allowed us to superimpose the anatomical connection results and physiological maps in the same plane. The hand/face border in area 3b was estimated by myelin staining and electrophysiological recordings.

SM-J (100% DCL)—CTB was injected into the hand region of area 3b that responded to touch on the hand and chin (~1.5 mm medial to the hand/face border). The location is comparable to the expected territory of digit 2 (Figs. 4A, 5A). The CTB injection core and dense uptake zones were primarily confined to the territory that had receptive fields in the hand and chin with slight spreading into surrounding areas that were unresponsive to touch on the hand, face, and forelimb. Two injections of BDA were made in the chin representation in area 3b, with the injection cores completely restricted within the boundary, ~1 mm lateral to the hand/face border (Figs. 4A, 5B).

Both CTB and BDA injections produced dense distributions of label across cortical regions (Fig. 5C). CTB-labeled neurons were primarily concentrated in the hand region of area 3b, slightly extending medially into the forelimb regions. Surprisingly, small numbers of CTB-labeled neurons were found beyond the hand/face border in the face region of area 3b. The extent of expansion was approximately 1.3 mm lateral to the hand/face border. CTB-labeled neurons appeared to be clustered into several small patches surrounding the injection site; however, such modularly arranged labeling patterns were not obvious after we superimposed the plots of multiple sections for illustration, as shown in Figure 5C. Caudally in area 1, a large number of CTB-labeled neurons clustered in the hand region that is medio-laterally parallel to the injection site in area 3b, and a similar pattern is also found in normal monkeys (Liao et al., 2013). Populations of CTB-labeled neurons were also present rostrally in areas 3a and M1, and in the cortex of the upper bank of the lateral sulcus, where PV and S2 are located. Although distributions of CTB-labeled neurons were denser in the hand regions in these areas, small numbers of labeled neurons spread into their face regions. In the S2/PV area, the distribution of CTB-labeled neurons extended rostrocaudally for approximately 4.5 mm. Scatterings of CTB-labeled neurons were also observed in area 2, the frontal cortex, and the expected territory of premotor dorsal and ventral areas (PMd and PMv; Gharbawie et al., 2011; Stepniewska et al., 2014) as well as two areas in the upper bank of the lateral sulcus: parietal rostral (PR) and retroinsular cortex (Ri). The BDA injection in the chin representation of area 3b labeled a large number of neurons primarily restricted to the face region of area 3b, with a slight spread into the hand region. Small numbers of BDA-labeled neurons were scattered in the face regions in area 1, area 3a, and M1, and PV/S2. Likewise, we observed BDA-labeled terminals primarily confined to the face region of areas 3b, 3a, 1, 2, and PV/S2. Sparse BDA-labeled terminals extended into the hand regions in areas 1, 2, 3a, M1, and PV/S2. Interestingly, we observed overlap of CTB-labeled neurons and BDA-labeled neurons and terminals in the face regions of areas 3b and PV/S2.

SM-U (86% DCL)—In monkey SM-U, BDA injection in the chin representation of the face region (~550 μm lateral to the hand/face border) in area 3b labeled neurons concentrated at the injection site in the face region of area 3b (Figs. 4B, 6). Only one neuron was found in the hand region near the hand/face border of area 3b (Fig. 6B). Few BDA-labeled neurons were observed in the face region of area 1. The BDA-labeled terminals mostly overlapped BDA-labeled neurons in the face regions of areas 3b and 1, and extended laterally to the face regions of PV/S2. A small amount of BDA-labeled terminals extended into an unidentified area in the cortex of the lower bank of the lateral sulcus.

SM-Y (65% DCL)—We made two injections of CTB into the electrophysiologically defined territory of digit 2 in the hand region in area 3b in monkey SM-Y (~1.3 and 1.7 mm medial to the hand/face border; Figs. 4C, 7A). The dense uptake zone was primarily located in the territory of the digit 2 representation, but slightly involved the representation of radial hand. Two BDA injections were made into the face cortex representing the chin and lower lip (~900 μm and 1.5 mm lateral to the hand/face border; Figs. 4C, 7B).

The labeled neurons and terminals from CTB and BDA injections were primarily distributed in the somatosensory cortex representing matching receptive fields, with a more widespread pattern (Fig. 7C). The population of CTB-labeled neurons was densest close to the injection site in the hand region of area 3b, and less dense in the surrounding cortex. However, there were some labeled neurons aggregating into a small cluster close to the tip of the central sulcus where representations of the forelimb were mapped, along with abnormally located D1 representations. A small number of labeled neurons spread laterally across the hand/face border into the face region in area 3b, with the farthest distance ~ 1.8 mm lateral to the hand/face border. In areas 1, 3a, M1, and PV/S2, large numbers of CTB-labeled neurons were mainly distributed in the hand regions, although a few labeled neurons were present in their face regions. The rostrocaudal extension of CTB-labeled neurons in PV/S2 was approximately 3 mm. We also identified patches of labeled neurons in the expected locations of PMv, Ri, the cortex of lower bank of the lateral sulcus where ventral somatosensory cortex (VS) is located (Coq et al., 2004; Cusick et al., 1989), and several unidentified areas in the frontal cortex and cortex of the lateral sulcus. A small number of CTB-labeled neurons were scattered in the expected location of PMd and PR. The BDA injection in the face region of area 3b produced a large number of labeled neurons and terminals within the face region in area 3b, with lower densities in areas 1, 3a, M1, and PV/S2. Unexpectedly, we observed BDA-labeled neurons and terminals expanding into the most lateral area of the hand region in area 3b. Such BDA-labeled neurons were mostly distributed in the area that was 300 μm medial to the hand/face border, and the farthest extent was approximately 1 mm from the border. Sparse BDA-labeled terminals even extended laterally into the hand regions of PV/S2, overlapping the CTB-labeled neurons.

SM-T (61% DCL)—CTB was injected into the representation of glabrous and dorsal parts of digit 2 in the hand region, with the core and dense uptake zone completely confined to the territory of digit 2 (~1.5 mm medial to the hand/face border; Figs. 4D, 8A). A focal injection of BDA was made in the representation of the chin in the face region of area 3b (~900 μm lateral to the hand/face border; Figs. 4D, 8B).

The population of CTB-labeled neurons was confined to hand regions of somatosensory cortical areas (Fig. 8C). As in other cases, CTB-labeled neurons were mostly concentrated at the injection site in area 3b, occasionally spreading into the face region of area 3b that is approximately 700 μm lateral to the hand/face border. No labeled neurons were found in the forelimb region. We noted small numbers of CTB-labeled neurons clustered in the medial and lateral aspects of the hand region in area 3b. Similar distributions of label were observed in areas 1, 3a, and M1. Small numbers of labeled neurons were present in the expected locations of area 2, PMd, PMv, supplementary motor area (SMA), and Ri, and several unidentified areas in the cortex of the lateral sulcus. CTB-labeled neurons were scattered in

the expected PR location. The CTB injection labeled a great number of neurons in the hand region of PV/S2 area, extending rostrocaudally for approximately 5 mm. The BDA injections in the face region of area 3b produced a small number of labeled neurons but extensive distributions of labeled terminals. The BDA-labeled neurons were mainly restricted to the face region of area 3b, overlapping the BDA-labeled terminals. The BDA-labeled terminals slightly extended into the most lateral aspect of the hand region in area 3b. We also observed patches of BDA-labeled terminals in the face regions of areas 1 and 2, and in PV/S2. Slight overlap of CTB-labeled neurons and BDA-labeled terminals was found at the borders between the regions of the face and hand in these areas.

Distributions of label in relation to reactivated somatotopy in area 3b and 1

We superimposed the distributions of CTB- and BDA-labeled neurons onto the topographic maps of the hand and face in areas 3b and 1 (Fig. 4) after long-standing DCLs (Figs. 5–8, lower row). We counted the numbers of labeled neurons in areas 3b and 1 and calculated the percentages of labeled neurons that overlapped the territories we estimated from electrophysiological mapping that were responsive to touch on hand, face, and forelimb, or were unresponsive (see Materials and Methods).

SM-J (100% DCL)—We identified a total of 8987 CTB-labeled neurons in the area 3b after CTB injection in the hand region in monkey SM-J, of which 96.9% were confined to the hand region (Fig. 5D). Although CTB injections were targeted at the expected location of digit 2 representation where the neurons recorded in this region had mixed receptive fields in the hand and face, only 10.6% of the labeled neurons overlapped the territory responsive to touch on both hand and face. However, 54% of CTB-labeled neurons overlapped the cortex that remained unresponsive to touch on hand, face and forelimb. Smaller percentages of labeled neurons in the hand region overlapped the responsive territories of multiple digits (10.7%), forelimb and face (15.7%), face (new face, 4.8%), forelimb (new forelimb, 0.5%) and forelimb and hand (0.2%). We identified 18 labeled neurons (0.2%) overlapping the forelimb region. A small population of CTB-labeled neurons (n = 284; 3.2%) was found in the face region of area 3b, mainly overlapping the representations of chin and lower lip. In area 1, we identified a total of 638 CTB-labeled neurons. These labeled neurons were mainly located in the hand region (n = 629; 98.2%), overlapping the unresponsive zone (97.8%). Only 9 labeled neurons (1.4%) overlapped the cortex responsive to taps on the hand. We noted 3 CTB-labeled neurons (0.5%) in the forelimb region and 9 labeled neurons (1.4%) in the face region of area 1.

The BDA injection labeled 3046 neurons in area 3b, of which 99.4% were within the face region (Fig. 5E). Only 16 BDA-labeled neurons (0.6%) extended medially at or across the hand/face border. Eleven of them overlapped the hand cortex that represented the face and hand, which was also innervated by BDA-labeled terminals (Fig. 5F). Only 6 BDA-labeled neurons were present in area 1, overlapping the unresponsive zones.

SM-U (86% DCL)—The BDA injection in the face region of area 3b labeled a total of 744 neurons in areas 3b and 1 in monkey SM-U (Fig. 6D). The BDA-labeled neurons were mostly concentrated at the chin representation, and less densely labeled in representations of

cheek and lower lip in area 3b. One BDA-labeled neuron was found beyond the hand/face border, overlapping the unresponsive zone. Only 6 labeled neurons were distributed in the face region of area 1. The BDA-labeled terminals primarily overlapped BDA-labeled neurons in the face regions in areas 3b and 1 (Fig. 6E).

SM-Y (65%)—A total of 12140 CTB-labeled neurons were identified in area 3b after CTB was injected into the hand region of area 3b (Fig. 7D). A large percentage of labeled neurons (99%) were located in the hand region, mainly overlapping the cortex responsive to touch on digit 2 (30.7%) and digit 1 (23.6%). Few CTB-labeled neurons were present in the medial location that had unexpected receptive fields in digits 1 and 2, and only 24 labeled neurons overlapped this reorganized cortex. CTB-labeled neurons medially overlapped the representations of digits 3 (4.7%) and 4 (2.6%) and caudally overlapped the representation of the palm (11.3%). A small percentage of labeled neurons (8.8%) overlapped the territory involving multiple digits and the dorsal hand. Other CTB-labeled neurons (17.3%) in the hand region overlapped unresponsive cortex. While 12 labeled neurons (0.1%) overlapped the forelimb region, we identified 124 CTB-labeled neurons (1.0%) in the face region. Caudally in area 1, a total of 1619 CTB-labeled neurons were found. A large percentage of labeled neurons (96.7%) were in the hand region, overlapping the cortex responsive to touch on digits 1 (3.0%), 2 (16.1%), 3 (0.8%), and 4 (0.8%). Populations of CTB-labeled neurons overlapped the representations of multiple digits or the dorsal hand (17.7%) and palm (20.6%). We found 610 CTB-labeled neurons (37.7%) overlapping the unresponsive zone in the hand region of area 1.

BDA injection in the face region of area 3b labeled a total of 3268 neurons within the territory area 3b (Fig. 7E). The majority of BDA-labeled neurons (96.9%) remained in the face region. However, we identified a small percentage of BDA-labeled neurons (3.0%) that expanded into the hand region primarily overlapping the digit 1 representation, which was also innervated by BDA-labeled terminals (Fig. 7F). Only 3 BDA-labeled neurons were scattered in area 1. Sparse BDA-labeled terminals were found in the territory of the hand region in area 3b.

SM-T (61%)—Superimposing plots of CTB- and BDA-labeled neurons on the somatotopic maps confirmed that connections of hand and face neurons of area 3b were confined to somatotopically-matched cortex in areas 3b and 1 in monkey SM-T. Dense distributions of CTB-labeled neurons in area 3b overlapped the representation of digit 2 (46.4 % of 12873 neurons; Fig. 8D), and distributions were less dense in the representation of digit 3 (19.2%). Small numbers of CTB-labeled neurons overlapped the representations of digits 1 (9.3%), 4 (8.1%), and 5 (0.1%), and the palm (10.8%). The clusters of labeled neurons outside the main population partially overlapped representations involving multiple digits (3.8%) or unresponsive zones (2.2%). Only 0.1% of CTB labeled neurons spread into the face region of area 3b in this case. In area 1, although CTB-labeled neurons were concentrated in the expected location of digit 2 representation, only 2.3% of labeled neurons overlapped the electrophysiologically defined representation of digit 2, and 11.2% overlapped the representation of the palm. Small populations of CTB-labeled neurons overlapped the representations of digits 4 (9.6%) and 5 (0.6%). The majority of CTB-labeled neurons

overlapped the unresponsive zones (82.4%). The majority of BDA-labeled neurons from the tracer injection in the representation of chin in area 3b overlapped the face region of area 3b (98.6% of 354 neurons; Fig. 8E), mainly the chin representation. Only 5 BDA-labeled neurons were found medially in the hand region, specifically the representation of digit 1 (0.8%) or unresponsive zones (0.6%), overlapping the most lateral region of the representations of digit 1 and the hand/face border. The distributions of BDA-labeled terminals were primarily confined to the face regions in areas 3b and 1, with slight spreading into the hand region of area 3b (Fig. 8F).

Statistical summaries—To investigate whether the connectional densities between somatotopic representations in the hand region of area 3b were altered after DCLs, results from the four monkeys in the present study were compared to the data obtained from two normal monkeys in our previous publication (Liao et al., 2013). We included these normal comparisons in figures 9 and 10 and in statistical analysis. The majority of the statistical tests were performed using the broad Response factors that indicated the territory and response type (see Materials and Methods). Results of the analysis using the subdivided categories are indicated separately. Specifically, for one analysis and for display purposes (Fig. 9), the 'Response' categories were subdivided based on mapping territories that responded to individual parts of the hand. We separated the statistical analysis by the type and location of the injections (CTB injection in the 3b hand region and BDA injection in the 3b face region). Differences in the tracer uptake may lead to apparent differences between the numbers and locations of labeled neurons. Thus, the results from each injection type were analyzed separately. Selected results are listed in the text (see more detailed statistics reported in Tables 3–4).

Statistical analyses of BDA label after face region injections—DCL would be expected to have limited direct effects on cortical connections involving the area 3b face representation. After regions representing the face in area 3b were injected with BDA in monkeys following DCL, the majority of labeled neurons were found in face region. However, a few neurons were labeled by BDA in digit territories, including digits 1 and 2, and we detected that differences in the percent of BDA-labeled neurons were significantly affected by the extent of lesion (DCL: $p < 0.0001$), such that increasing the extent of the DCL increased the proportions of neurons that were labeled within the hand region, and particularly regions that were not responsive to touch or that responded to touch on multiple locations (e.g., both hand and face responses from the same microelectrode recording). The analysis also confirmed that after injections into the area 3b face region, larger proportions of labeled neurons were found in area 3b compared to area 1 (Area: $p < 0.0001$). As expected, the majority of BDA-labeled neurons in areas 3b and 1 were located in the face region, with fewer neurons labeled in the hand and/or forelimb regions (Response: $p < 0.0001$). The statistical modeling analysis also detected interactions between those main effects (DCL × Area: $p < 0.0001$; DCL × Response: $p < 0.0001$; DCL × Area × Response: $p < 0.0001$).

Table 3 provides a subset of the statistical results for area 3b (area 1 not shown) to indicate the comparisons of the percentages of labeled neurons in the broad response territories (e.g.,

forelimb, hand) for monkeys with different DCL extents. The values for the percentages of labeled neurons in the selected response subdivisions are also included. The large numbers of pairwise comparisons with significant differences prevented us from including indicators of statistical comparisons in Figure 9A. After the BDA face region injections, small numbers of neurons were labeled in the hand region of area 3b. Labeled neurons were found in the representations of digits 1 and 2 as well as other regions in area 3b. However, differences based on the DCL extent could not be detected statistically between the proportions of neurons labeled within the subdivided parts of the hand region (e.g., D1, D2; see Fig. 9A),

Statistical analyses of CTB label after hand region injections—Our results indicated that the differences in the patterns of CTB-labeled neurons overlapping the altered somatotopic representations in areas 3b and 1 (Fig. 9B, C) overall were significantly affected by the extent of the lesion (DCL: $p < 0.0001$). Figure 9 (B, C) shows the percentages of CTB-labeled neurons in specific response regions of areas 3b and 1 following the CTB injections in the area 3b hand region associated with digit 2. Note, case SM-U (86% DCL) was not included in the analysis due to lack of CTB label (possibly caused by blockage of the injection pipette). However, we included data from two monkeys with no spinal cord lesions for comparisons (Liao et al., 2013). In these two cases without lesions, the percentages of labeled neurons in somatotopic representations of the hand in area 3b were obtained from superimposing the plots on the electrophysiologically defined maps (Fig. 9B blue), with the same methods used for the monkeys with DCLs. However, for area 1 in the two cases without lesions, the percentages of labeled neurons in the hand region were obtained from superimposing the plots on the estimated borders of digits representations based on widely accepted somatotopic maps in squirrel monkeys (Sur et al., 1982; Fig. 9C blue). Figure 9 shows the percentage of labeled neurons found in selected somatotopic regions for individual cases with DCLs; therefore, for visualization purposes the highest values from one case without the DCL are shown. However, for statistical analysis, the values for both monkeys without DCLs were included (rather than a maximum as shown in Fig. 9B, C or a mean value).

CTB injection in the area 3b hand region of monkeys without DCL resulted in greater percentages of neurons labeled in area 1 overall (Area: $p < 0.0001$), which may be due in part to dense uptake zones in area 3b. As expected, the majority of CTB-labeled neurons in areas 3b and 1 corresponded to the hand region, with fewer neurons labeled in the face and/or forelimb regions (Response: $p < 0.0001$). The interactions between those main effects were significant contributors to differences in the percentages of labeled neurons (DCL × Area: $p < 0.0001$; DCL × Response: $p < 0.0001$; DCL × Area × Response: $p < 0.0001$). Table 4 provides a subset of the statistical results for area 3b to indicate the comparisons of the percentages of labeled neurons in the broad response territories and the values for the percentages of labeled neurons in the selected response subdivisions for normal and DCL monkeys. The large numbers of pairwise comparisons with significant differences prevented us from including indicators of statistical comparisons in Figure 9B, C.

We also examined the specific response territories for parts of the hand (digit 1 instead of Hand, etc.) to evaluate possible differences in the distributions of label, and the percentages of neurons labeled in these response territories in area 3b after CTB injections are indicated

in Figure 9B. Territory in area 3b that was responsive to touch on digit 5 was labeled after CTB injection in the digit 2 representation for the cases with no lesion and the least extensive lesion (61% DCL) with similar percentages (0.148%, 0.147%). This observation indicates that widespread anatomical connections between digit representations occur normally and such connections were maintained in the case with the least severe injury, but not in the cases with extensive lesions. Connections between the digit 2 representation and territory responsive to digit 4 was labeled in all cases except SM-J (100% DCL), from which responses to touch on individual digits were rarely encountered, and the percentages of labeled neurons were greater in SM-T (61% DCL: 8.1%) and SM-Y (65% DCL: 2.6%) than for the cases without lesions (mean = 0.7, N = 2). We detected differences in the labeling of territory responsive to digit 1 such that the percentage of labeled neurons in SM-Y (65% DCL: 23.6%) was more than double the mean percentage for the cases without lesions (10.3%) and SM-T (61% DCL: 9.3%). This doubling may relate to the expansion of the territory responsive to digit 1 in SM-Y that had the DCL at the C5/C6 level (65% DCL).

Within area 3b, the neurons labeled by CTB injection in the hand (digit 2) representation were largely found in the hand region of area 3b. We found trends such that the more extensive the lesion, the greater percentage of labeled neurons were found in ‘expected hand regions’ that were unresponsive to touch on the hand, face, and/ or forelimb during somatotopic mapping (Fig. 10 Hand, NR; 0% No lesion: 0 labeled neurons; 61% DCL: 2.2%; 65% DCL: 17.3%; 100% DCL: 54%). This trend is illustrated by the stacked bar chart in Figure 10. Trends of the increased percentages of labeled neurons in the face region were also shown in more extensive lesioned cases (0% No lesion: 0 labeled neurons; 61% DCL: 0.1%; 65% DCL: 1%; 100% DCL: 3.2%). However, small percentages of CTB-labeled neurons were found in the forelimb region in normal (0.6%) and DCL cases (61% DCL: 0%; 65% DCL: 0.1%; 100% DCL: 0.2%). Note, the values representing the two normal monkeys in Figure 10 were calculated from the weighted average of the neuron counts for the two normal monkeys.

Relationships between injection site and labeled regions—Lesion extent significantly affected the proportion of neurons that were labeled in regions outside of the expected territories of the hand or face. While cases with no lesions did not show mismatches of the injection site and labeled zones, all DCL cases had neurons labeled in zones that did not match the injection site ($p < 0.0001$). When only the injection into the hand region was considered, the difference was still detected ($p = 0.013$). Additionally, only the most extensive lesion case was found to have labeled neurons in regions responsive to two or more different body parts (e.g., forelimb and face), which distinguished the 100% DCL case from other cases overall ($p < 0.0001$) and when only the injection into the hand region was considered ($p < 0.0001$).

Distributions of neurons projecting to area 3b in the thalamus

To reveal the organization of thalamocortical projections after DCLs, we plotted the distributions of labeled neurons and terminals in VP from tracer injections in the ipsilateral area 3b (Fig. 11). In monkey SM-J that had a complete DCL (Fig. 11A–C), CTB injection in the expected digit 2 representation in area 3b labeled neurons and terminals primarily

restricted to the territory of digit 2 in the VPL. We determined this by superimposing the plotting of labeled neurons to adjacent sections stained for CO (Qi et al., 2011). CTB-labeled neurons were occasionally observed in the digit 1 representation in VPL. Small numbers of CTB-labeled neurons were found in the ventroposterior superior nucleus (VPS; Cusick et al., 1985). Likewise, BDA injection in the chin representation in area 3b labeled neurons in the most lateroventral aspect of ventroposterior medial nucleus (VPM). We identified small and large BDA-labeled terminals within the territory of VPM, extending ventrally into the ventroposterior inferior nucleus (VPI).

In monkey SM-Y with an incomplete DCL (65% complete), CTB injections in the hand region of area 3b that primarily involved the representation of digit 2 with minor spread into the representation of digit 1, labeled neurons and terminals mostly in the representations of digits 1 and 2 in VPL (Fig. 11D–F). A small number of CTB-labeled neurons spread laterally into the territories of digits 3–4 in VPL. BDA-labeled neurons were again confined to VPM. Small BDA-labeled terminals overlapped the BDA-labeled neurons and extended into VPS and VPI. Clusters of large BDA-labeled terminals were present in VPI and VPS. Similar patterns of CTB- and BDA-label in the VP were shown in monkey SM-T (61% complete) after CTB and BDA were injected into the hand and face regions, respectively, in area 3b (not shown). CTB-labeled neurons and terminals were completely restricted to the representation of digit 2 in VPL, whereas BDA-labeled neurons and terminals were in the territory of VPM. We did not find BDA-labeled neurons or terminals in the VP in monkey SM-U, possibly due to the small and inefficient BDA injection in the cortex.

Our findings revealed that thalamocortical projections from VPM and VPL to area 3b primarily retained a normal somatotopically-matched pattern. However, an incomplete DCL at the cervical spinal cord may disrupt the somatotopically restricted connections from representations of digits in the VPL to area 3b.

Peripheral projections from face to first relay nucleus in the brainstem

We examined the terminations of face inputs at the brainstem level by injecting B-HRP into the anterior chin ipsilateral to the DCL site (Fig. 12A). A large, dense patch of terminals were labeled with B-HRP in the most dorsal aspect of the trigeminal nucleus in the four DCL monkeys (see examples in Fig. 12, white arrowheads). However, we found sparse B-HRP-labeled terminals in the Cu approximately 1.5 mm caudal to the obex in the monkey, SM-J, that received a complete DCL at C4 (Fig. 12C, red arrows), suggesting that face inputs expanded into the hand nucleus at the level of brainstem (Jain et al., 2000). However, in the other three monkeys that received incomplete DCLs, B-HRP- labeled terminals were completely restricted to the territory of the trigeminal nucleus, no terminals were found in the Cu of brainstem (Fig. 11C).

DISCUSSION

In the present study, we determined the connection patterns of neurons in the hand and face regions of area 3b in squirrel monkeys months after a sensory loss produced by cutting ascending sensory axons in the contralateral dorsal column pathway. Although the intrinsic connection patterns, feedback connections with areas 1, 3a, M1, and PV/S2, and the

connections with the VPL closely resembled the connection patterns revealed in normal monkeys (Burton and Fabri, 1995; Liao et al., 2013; Negyessy et al., 2013; Qi et al., 2011b), some differences were noted. First, small numbers of neurons were found to project from the hand region to the face region, and from the face region to the hand region of area 3b. Neuron connections rarely cross the hand/face border in normal monkeys (Fang et al., 2002; Liao et al., 2013). In addition, the intrinsic connections labeled within the hand region of area 3b appeared to be more widespread in the cases with incomplete DCLs than in a case with a complete lesion, or in previous cases of intact squirrel monkeys. Thus, some limited amounts of sprouting and growth of area 3b intrinsic connections likely occurred. Also, as the cortical reactivation of the hand region of cortex was more limited in the case with the complete DCL and some of the reactivation was from the face, intrinsic connections included territories responsive to touch on the face, or to the face and hand, as well as hand alone, possibly promoting perceptional errors (Ramachandran et al., 1992; Rausell et al., 1998). In those monkeys with incomplete DCLs, intrinsic connections tended to relate to cortex activated by touch on the hand. Second, feedback connections from areas 3a, 1, M1, and PV/S2 to the hand region of area 3b tended to be more widespread in lesioned monkeys, and included feedback projections from regions representing the face. These somatotopically mismatched feedback connections (compared to normal somatotopic organization) may contribute to an activation of hand cortex by stimuli on the face. Our results are described further below and summarized in Figure 13.

Intrinsic connections in the area 3b after DCLs

The hand region of area 3b—In primates, the intrinsic connections of neurons in the hand representation in area 3b are normally concentrated around the injection site, with progressively reduced connections to other parts of the hand region (Burton and Fabri, 1995; Fang et al., 2002; Liao et al., 2013; Negyessy et al., 2013). Few or no neurons in the hand region of area 3b connect to cortex representing the face or forelimb. In a similar manner, the labeled neurons in the present DCL monkeys were mostly concentrated around the injection site, with reduced numbers in surrounding cortex. Yet, while neurons in the representation of digit 2 of area 3b have denser connections to the representation of digit 3 than to representations of other digits and the palm in normal monkeys (Liao et al., 2013), in these DCL cases, the connection densities from the reactivated representations within the hand region differed somewhat from that observed in normal monkeys.

In monkey SM-J that had a complete DCL, the intrinsic connections of area 3b hand neurons served to integrate the weakly reactivated hand inputs and new inputs from face and forelimb. Results from monkeys SM-Y and SM-T, which had similar amounts of deprived axons from the hand, could reflect how the differences in remaining hand inputs altered the functional connectivity within area 3b. In monkey SM-T that lost partial inputs from digits 1–5 (61% DCL), we observed a nearly normal somatotopic organization in area 3b after long-term recovery. Area 3b neurons responsive to touch on the digit 2 had remarkably denser connections with neurons responsive to digit 3 when compared to neurons in representations of digit 1 and other parts of hand, resembling normal patterns (Liao et al., 2013). However, in monkey SM-Y, which retained inputs from digit 1 and a portion of digit 2 but lost most inputs from digits 3–5 (65% DCL), territories of digits 1 and 2 were

obviously larger in area than those of digits 3–5 and expanded medially. Digit 2 neurons had denser connections to neurons in the representations of digit 1, adjacent palm, and the caudal unresponsive zone than to those in the representations of digits 3–4. Although the CTB injection site was near the medial border of the digit 1 representation, the injection core did not spread into the representation of digit 1 (see Fig. 4), and the location of the medial border of the digit 1 representation possibly resulted from territory expansion after injuries. The altered pattern likely reflected widespread connections that integrate the remaining inputs from digits 1 and 2 in monkey SM-Y. We speculate that the remaining inputs from the hand provide essential sensory feedback for touch, promote hand use after injuries, and strengthen the connection densities within the reactivated hand territory in the somatosensory cortex. We also noted additional patches of labeled neurons in the medial and lateral aspects of the hand region in incomplete DCL monkeys SM-Y and SM-T. Although this labeling resembles distributions in monkeys without lesions (Liao et al., 2013; Negyessy et al., 2013), the partial overlap with the territories responsive to touch on digit 1 (in SM-Y) and multiple digits (in SM-T) suggests the formation of new connections providing inputs to the deprived hand neurons (Florence et al., 1998).

Interconnections cross hand/face border in area 3b—Intrinsic connections across the hand/face border in area 3b in the present cases clearly reveal that connectional plasticity occurred after DCLs. This is because the hand/face border in area 3b of primate monkeys can be physiologically and histologically distinguished (Cerkevich et al., 2014; Fang et al., 2002; Jain et al., 1998; Merzenich et al., 1984; Qi and Kaas, 2004; Wall and Kaas, 1986), and the intrinsic connections of area 3b neurons rarely cross the border in normal monkeys (Burton and Fabri, 1995; Fang et al., 2002), with one known exception. Manger et al. (1997) reported that tracer injections in the representation of lower jaw/neck in area 3b of macaque monkeys, which is anatomically located between the hand and face regions, labeled neurons and terminals in the representations of digit 1 and its connecting thenar palm, suggesting that neurons near the hand/face border normally have reciprocal connections to digit 1 neurons. Because of the possibility of contaminating the border region by injections, we avoided injecting tracers near the border. Our data were obtained from tracer injections in the expected location of digit 2 representations or the chin representation in area 3b, and we found that the DCLs resulted in sprouting of connections beyond the border of the injected region.

Fang et al. (2002) quantified the ratio of connections across the hand/face border by tracer injections into the representations of digit 2 and chin of area 3b in normal New World squirrel monkeys, owl monkeys, and marmosets. Their results showed that only 0.01% connections extended across the hand/face border in area 3b. In monkeys after long-term DCL, we found that injections of CTB into the representation of digit 2 in area 3b labeled more neurons spreading past this border. The extent of connections of the digit 2 neurons beyond the border is approximately 1.5 mm. Although our data did not reveal linear correlations between ratios of cross-regional connections and the severity and level of DCLs, the DCLs differed when comparing the presence of cross-regional connections and comparing the presence of labeled neurons in regions that responded to touch on more than one body part. In monkey SM-J with the most extensive lesion (100% DCL), 3.2% of hand

connections from the digit 2 territory in area 3b expanded into the face region. After the most restricted lesion studied here in monkey SM-T (~61% DCL), 0.1% of hand connections spread into the face region. Likewise, we observed a slight expansion of face connections (0.6%-3.1%) into the hand region after BDA was injected in the representation of chin in area 3b in these monkeys. The findings of both CTB- and BDA-labeled neurons beyond the hand/face border suggest that area 3b neurons can form reciprocal connections across the regional border after peripheral sensory loss, and that these connections contribute to the presence of neurons in the hand region of area 3b that became responsive to touch on the face.

Intracortical connections to other somatosensory cortical areas

Feedback projections to hand and face regions of area 3b from other cortical areas mostly corresponded to a normal, somatotopically-matched pattern, but more widespread connections were present in several cortical areas including areas 3a, 1, 2, M1, PV/S2, the expected location of PMv, and several unidentified areas in the cortex of the lateral sulcus after DCLs in squirrel monkeys. Such connections may provide inputs from other somatosensory pathways to the affected neurons in area 3b, consequently modulating the cortical reactivation in the deprived region of area 3b after DCLs. Here we compare the distributions of feedback connections from each cortical area to early studies with normal monkeys (Burton and Fabri, 1995; Liao et al., 2013; Manger et al., 1997; Negyessy et al., 2013).

Area 1—Layer 4 neurons of area 1 receive corticocortical inputs from layer 2–3 of area 3b (Garraghty et al., 1990a; Vogt and Pandya, 1978), and layer 3 neurons receive small amounts of thalamocortical inputs from VP (Jones, 1975; Jones and Powell, 1970; Lin et al., 1979; Nelson and Kaas, 1981). Previous studies showed that connections between areas 3b and 1 are largely somatotopically matched (Ashaber et al., 2014; Burton and Fabri, 1995; Cusick et al., 1985; Liao et al., 2013; Negyessy et al., 2013), but neurons in area 1 have larger receptive fields and more complex response properties (Sur et al., 1982). Area 1 normally depends on area 3b for activation (Garraghty et al., 1990a). In DCL monkeys, we found that most of the area 1 hand neurons remained unresponsive to touch on hand, forelimb, or face after DCLs, which is likely due to reduced activation of inputs from area 3b, together with the greater effect of anesthesia on non-primary areas of cortex. However, CTB injections in the hand region of area 3b continued to label large numbers of neurons in the expected location in the hand region of area 1, although the majority of the labeled neurons were within the unresponsive cortex.

Along with the expected pre-existing connections, additional patches of CTB-labeled neurons in area 1 were observed in monkeys SM-Y and SM-T, which had incomplete DCLs, but not in monkey SM-J, which completely lost hand inputs via the dorsal column pathway. These observations suggest that remaining dorsal column inputs may facilitate the formation of new connections from area 1 to area 3b, possibly promoting the recovery of cortical activity in area 3b. While a scattering of projections from neurons in the face region of area 1 to the reactivated hand region of area 3b were found (1.4%-3.0%), anterograde and

retrograde connections of the chin representation in area 3b remained restricted to the face region of area 1.

Areas 3a and 2—Both areas 3a and 2 are known to carry proprioceptive inputs via thalamocortical projections from the region superior to VP, the VPS (Cusick et al., 1985; Kaas et al., 1984; Lin et al., 1979; Nelson and Kaas, 1981; Pons and Kaas, 1985) or the anterodorsal shell of ventrobasal complex (Friedman and Jones, 1981; Jones and Friedman, 1982). Both areas 3a and 2 receive cutaneous information from areas 3b and 1 (DeFelipe et al., 1986; Jones et al., 1978; Pons and Kaas, 1986; Shanks et al., 1985). Accordingly, DCLs may deprive a portion of activating inputs to areas 3a and 2. We again found that hand and face regions in area 3b retained dense connections to somatotopically-matched regions in area 3a after DCLs, even though the area 3b hand injection labeled neurons in a more widespread pattern in the hand region of area 3a, and small numbers of labeled neurons spread into the face region in area 3a. A similar connection pattern was also seen from area 2 to area 3b, although with much less density.

Areas PV/S2 and other cortical areas in lateral sulcus—PV and S2 are located in the cortex of the upper bank of the lateral sulcus, and their activations are dependent on feedforward projections from area 3b (Burton et al., 1990; Disbrow et al., 2003; Garraghty et al., 1990b; Jones et al., 1978; Pons et al., 1992). In addition, PV/S2 receives thalamocortical projections from the VPI (Friedman and Murray, 1986; Jones and Powell, 1970; Krubitzer and Kaas, 1992; Qi et al., 2002), which is driven by spinothalamic inputs (Craig and Zhang, 2006; Shi and Apkarian, 1995). Thus, DCLs deprive a large portion of PV/S2 of activating inputs, but important inputs from the spinothalamic system remain. In the DCL cases, neurons in PV/S2 were densely connected with the hand and face regions of area 3b, with a notable expansion of the PV/S2 region projecting to the hand region of area 3b. In normal monkeys, CTB injections in the digit 2 representation of area 3b usually labeled neurons in PV/S2 with a rostrocaudal extension of approximately 3 mm (Liao et al., 2013). However, the distribution of CTB-labeled neurons in PV/S2 in the injured monkeys in the present study extended rostrocaudally approximately 3–5 mm, possibly overlapping the representations of forelimbs and shoulder in PV/S2 (Coq et al., 2004; Disbrow et al., 2003). Further, slight overlap of CTB-labeled neurons and BDA-labeled terminals was observed at the expected border of hand and face regions of PV/S2 in monkey SM-T, which had a less severe DCL. In addition, we noticed an obvious overlap of CTB- and BDA-labeled neurons and BDA-labeled terminals in the face region of PV/S2 in monkeys SM-J and SM-Y, which had severe DCLs. Also, patches of BDA-labeled terminals extended into the hand region of PV/S2. Together, these observations suggest that after DCLs the feedback connections from the PV/S2 region to the hand region of area 3b increase to include mismatched feedback from neurons representing the face.

Extensive connections from other locations in the cortex of the lateral sulcus to the deprived hand region in area 3b were also shown in injured monkeys. Included areas are PR, VS and Ri (Coq et al., 2004; Cusick et al., 1985), and several yet to be defined areas in the rostral and caudal regions. Some of these connections also exist in normal monkeys (Liao et al.,

2013); however, more widespread connections were found in the DCL cases in the current study.

How do cortex, thalamus and brainstem contribute to the cortical reactivation after sensory loss?

We still do not fully understand how subcortical or cortical connections contribute to the reactivation in the deprived somatosensory cortex after peripheral sensory loss. Our present findings suggest that the organization of intracortical connections of area 3b neurons is more widespread after long-standing DCLs, although area 3b hand and face neurons remained densely and somatotopically connected within area 3b and to other somatosensory areas, similar to cases without lesions. The distributions of altered connections did not completely overlap the reorganized somatotopy in areas 3b and 1, revealing that intracortical connections of area 3b may not be the key source of the cortical reactivation after DCLs. However, we cannot exclude the possibility that the intracortical connections of area 3b neurons contribute to the reactivation of area 3b by increasing in synaptic strengths and numbers, especially by those neurons responsive to the intact inputs from the face and those from the hand that became effective in area 3b.

We did not observe large-scale expansion of connections as has been reported for area 1 hand neurons after hand amputation in macaque monkeys (Florence et al., 1998). While hand amputations remove all peripheral inputs from the hand, DCLs allow hand inputs to ascend to the somatosensory system through the spared dorsal column fibers and the second order spinal cord pathway (Liao et al., 2015). We speculate that such surviving hand inputs may promote the use of the affected hand sooner after sensory loss (Martinez et al., 2009; Qi et al., 2013) and restrict the formation of new connections within the hand region of each hierarchical station to area 3b and to other somatosensory cortex, consequently restricting the scale of anatomical rewiring. As we show that some reactivation by tactile afferents from the hand occurs in area 3b even after a complete DCL, the second order neurons that survive DCLs are the likely sources of this limited activation by relaying tactile information to the Cu (Liao et al., 2015). These second order spinal cord inputs to the Cu may increase or at least become more effective after DCLs.

In the present study, we found that CTB and BDA injections that mainly involved the representations of digit 2 and chin in area 3b labeled neurons separately in the VPL and VPM in all DCL monkeys. In monkey SM-J (100% DCL), the labeled neurons were narrowly clustered in the representation of digit 2 that was revealed by CO staining. The lack of labeled neurons in abnormal locations in VPM provides direct evidence that an anatomical reorganization of thalamocortical projections does not always play a significant role in mediating cortical reactivation after DCLs. Of course it is possible that the preserved thalamocortical connections may bring in reorganized inputs from the cuneate nucleus, as described in rodents (Li et al., 2014) and monkeys (Jain et al., 2000; present results). However, we observed a more widespread labeling in the representations of digits 3–4 in VPL in monkey SM-Y (65% DCL) after a digit 2 injection in area 3b, suggesting that the thalamocortical projections may sprout and not completely conform to the normal, somatotopically-matched pattern after injuries.

Our results from the brainstem provide further support for the hypothesis that brainstem plasticity guides at least some of the cortical reactivation after DCLs. In monkey SM-J with face representations in the reactivated hand region in area 3b, we found that B-HRP injections in the skin of the face labeled a small number of axonal terminals in the Cu of the brainstem, while tracer injections in the hand and face regions in area 3b labeled neurons primarily in normal patterns in the cortex and VP (Jain et al., 2000). In the other three monkeys, face afferents did not sprout into the Cu, nor did reactivated area 3b hand cortex respond to touch on face. One recent study by Kambi et al. (2014) provided strong evidence in support of this hypothesis. The authors first deprived the hand region in area 3b by making complete DCLs in the cervical spinal cord in macaque monkeys. As expected, new face inputs were found in the deprived hand region of area 3b after 14 months of recovery. The new representation of the face in the hand territory of area 3b was inhibited by inactivating the Cu, but inactivating the typical face territory of the area 3b did not affect the new face representation in hand territory. The findings strongly suggest that the brainstem is the key station in providing new activating inputs to part of the deprived cortex after injuries. However, we also observed a representation of face in the reactivated hand region in area 3a in monkey SM-U (see Fig. 4B), even though no labeled terminals were found in the Cu after face injections, suggesting that other somatosensory pathways may mediate cortical reactivations by the face after sensory loss in hand cortex, including direct connections across the hand/face border in area 3b.

In summary, our present findings indicate that the organization of intracortical connections of area 3b is anatomically altered by forming more widespread connections within area 3b and to other somatosensory cortex after long-standing DCLs. This expansion of connections was more obvious in monkeys with incomplete DCLs, suggesting that spared dorsal column inputs facilitate the formation of new corticocortical connections to area 3b hand neurons. We speculate that the preserved and expanded connections provide a substrate integrating surviving inputs from the periphery after injuries. In addition, our system-wide observations of connectional plasticity at cortical, thalamic, and brainstem levels suggest that changes in brainstem connections initiate the progression of reactivation, and the connections at thalamus and cortex serve to integrate the reactivating inputs for functional recovery.

ACKNOWLEDGEMENTS

We are grateful to Laura Trice for help with histological procedures; Mary Feurtado for surgical assistance; Barbara O'Brien, Emily Rockoff, Daniel Miller, Eva Sawyer and Drs. Omar Gharbawie, Denis Matrov, Christina Cerkervich, for data collection assistance.

ROLE OF AUTHORS: Study concept and design: C.C.L, J.L.R., J.H.K., H.X.Q. Acquisition of data: C.C.L, J.L.R., H.X.Q. Analysis and interpretation of data: C.C.L, J.L.R., J.H.K., H.X.Q. Drafting of the article: C.C.L., J.L.R. Obtained funding: J.L.R., J.H.K., H.X.Q. All authors edited and approved the manuscript.

Funding: This study is supported by NIH grant NS067017 to H.X.Q., NIH grant (NS16446) to J.H.K., and the Craig H. Neilsen Foundation (314739) to J.L.R and J.H.K.

LITERATURE CITED

Ashaber M, Palfi E, Friedman RM, Palmer C, Jakli B, Chen LM, Kantor O, Roe AW, Negyessy L. Connectivity of somatosensory cortical area 1 forms an anatomical substrate for the emergence of

multifinger receptive fields and complex feature selectivity in the squirrel monkey (Saimiri sciureus). J Comp Neurol. 2014; 522(8):1769–1785. [PubMed: 24214200]

Balaram P, Hackett TA, Kaas JH. Differential expression of vesicular glutamate transporters 1 and 2 may identify distinct modes of glutamatergic transmission in the macaque visual system. J Chem Neuroanat. 2013; 50–51:21–38. [PubMed: 19594444]

Balaram P, Kaas JH. Towards a unified scheme of cortical lamination for primary visual cortex across primates: insights from NeuN and VGLUT2 immunoreactivity. Front Neuroanat. 2014; 8:81. [PubMed: 25177277]

Baldwin MK, Balaram P, Kaas JH. Projections of the superior colliculus to the pulvinar in prosimian galagos (Otolemur garnettii) and VGLUT2 staining of the visual pulvinar. J Comp Neurol. 2013; 521(7):1664–1682. [PubMed: 23124867]

Burton H, Fabri M. Ipsilateral intracortical connections of physiologically defined cutaneous representations in areas 3b and 1 of macaque monkeys: projections in the vicinity of the central sulcus. J Comp Neurol. 1995; 355(4):508–538. [PubMed: 7636029]

Burton H, Sathian K, Shao DH. Altered responses to cutaneous stimuli in the second somatosensory cortex following lesions of the postcentral gyrus in infant and juvenile macaques. J Comp Neurol. 1990; 291(3):395–414. [PubMed: 2298940]

Cerkevich CM, Qi HX, Kaas JH. Corticocortical projections to representations of the teeth, tongue, and face in somatosensory area 3b of macaques. J Comp Neurol. 2014; 522(3):546–572. [PubMed: 23853118]

Chen LM, Qi HX, Kaas JH. Dynamic reorganization of digit representations in somatosensory cortex of nonhuman primates after spinal cord injury. J Neurosci. 2012; 32(42):14649–14663. [PubMed: 23077051]

Coq JO, Qi H, Collins CE, Kaas JH. Anatomical and functional organization of somatosensory areas of the lateral fissure of the New World titi monkey (Callicebus moloch). J Comp Neurol. 2004; 476(4):363–387. [PubMed: 15282711]

Craig AD, Zhang ET. Retrograde analyses of spinothalamic projections in the macaque monkey: input to posterolateral thalamus. J Comp Neurol. 2006; 499(6):953–964. [PubMed: 17072831]

Cusick CG, Steindler DA, Kaas JH. Corticocortical and collateral thalamocortical connections of postcentral somatosensory cortical areas in squirrel monkeys: a double-labeling study with radiolabeled wheatgerm agglutinin and wheatgerm agglutinin conjugated to horseradish peroxidase. Somatosens Res. 1985; 3(1):1–31. [PubMed: 4070891]

Cusick CG, Wall JT, Felleman DJ, Kaas JH. Somatotopic organization of the lateral sulcus of owl monkeys: area 3b, S-II, and a ventral somatosensory area. J Comp Neurol. 1989; 282(2):169–190. [PubMed: 2496153]

DeFelipe J, Conley M, Jones EG. Long-range focal collateralization of axons arising from corticocortical cells in monkey sensory-motor cortex. J Neurosci. 1986; 6(12):3749–3766. [PubMed: 2432205]

Disbrow E, Litinas E, Recanzone GH, Padberg J, Krubitzer L. Cortical connections of the second somatosensory area and the parietal ventral area in macaque monkeys. J Comp Neurol. 2003; 462(4):382–399. [PubMed: 12811808]

Fang PC, Jain N, Kaas JH. Few intrinsic connections cross the hand-face border of area 3b of New World monkeys. J Comp Neurol. 2002; 454(3):310–319. [PubMed: 12442321]

Felleman DJ, Van Essen DC. Distributed hierarchical processing in the primate cerebral cortex. Cereb Cortex. 1991; 1(1):1–47. [PubMed: 1822724]

Florence SL, Taub HB, Kaas JH. Large-scale sprouting of cortical connections after peripheral injury in adult macaque monkeys. Science. 1998; 282(5391):1117–1121. [PubMed: 9804549]

Florence SL, Wall JT, Kaas JH. Somatotopic organization of inputs from the hand to the spinal gray and cuneate nucleus of monkeys with observations on the cuneate nucleus of humans. J Comp Neurol. 1989; 286(1):48–70. [PubMed: 2475533]

Florence SL, Wall JT, Kaas JH. Central projections from the skin of the hand in squirrel monkeys. J Comp Neurol. 1991; 311(4):563–578. [PubMed: 1721925]

Friedman DP, Jones EG. Thalamic input to areas 3a and 2 in monkeys. J Neurophysiol. 1981; 45(1): 59–85. [PubMed: 7205345]

Friedman DP, Murray EA. Thalamic connectivity of the second somatosensory area and neighboring somatosensory fields of the lateral sulcus of the macaque. J Comp Neurol. 1986; 252(3):348–373. [PubMed: 3793981]

Garraghty PE, Florence SL, Kaas JH. Ablations of areas 3a and 3b of monkey somatosensory cortex abolish cutaneous responsivity in area 1. Brain Res. 1990a; 528(1):165–169. [PubMed: 2245335]

Garraghty PE, Pons TP, Kaas JH. Ablations of areas 3b (SI proper) and 3a of somatosensory cortex in marmosets deactivate the second and parietal ventral somatosensory areas. Somatosens Mot Res. 1990b; 7(2):125–135. [PubMed: 2116056]

Gharbawie OA, Stepniewska I, Kaas JH. Cortical Connections of Functional Zones in Posterior Parietal Cortex and Frontal Cortex Motor Regions in New World Monkeys. Cereb Cortex. 2011

Gibson AR, Hansma DI, Houk JC, Robinson FR. A sensitive low artifact TMB procedure for the demonstration of WGA-HRP in the CNS. Brain Res. 1984; 298(2):235–241. [PubMed: 6202368]

Imura K, Rockland KS. Giant neurons in the macaque pulvinar: a distinct relay subpopulation. Front Neuroanat. 2007; 1:2. [PubMed: 18958196]

Jain N, Catania KC, Kaas JH. Deactivation and reactivation of somatosensory cortex after dorsal spinal cord injury. Nature. 1997; 386(6624):495–498. [PubMed: 9087408]

Jain N, Catania KC, Kaas JH. A histologically visible representation of the fingers and palm in primate area 3b and its immutability following long-term deafferentations. Cereb Cortex. 1998; 8(3):227–236. [PubMed: 9617917]

Jain N, Florence SL, Qi HX, Kaas JH. Growth of new brainstem connections in adult monkeys with massive sensory loss. Proc Natl Acad Sci U S A. 2000; 97(10):5546–5550. [PubMed: 10779564]

Jain N, Qi HX, Catania KC, Kaas JH. Anatomic correlates of the face and oral cavity representations in the somatosensory cortical area 3b of monkeys. J Comp Neurol. 2001; 429(3):455–468. [PubMed: 11116231]

Jain N, Qi HX, Collins CE, Kaas JH. Large-scale reorganization in the somatosensory cortex and thalamus after sensory loss in macaque monkeys. J Neurosci. 2008; 28(43):11042–11060. [PubMed: 18945912]

Jones EG. Lamination and differential distribution of thalamic afferents within the sensory-motor cortex of the squirrel monkey. J Comp Neurol. 1975; 160(2):167–203. [PubMed: 803517]

Jones EG, Coulter JD, Hendry SH. Intracortical connectivity of architectonic fields in the somatic sensory, motor and parietal cortex of monkeys. J Comp Neurol. 1978; 181(2):291–347. [PubMed: 99458]

Jones EG, Friedman DP. Projection pattern of functional components of thalamic ventrobasal complex on monkey somatosensory cortex. Journal of neurophysiology. 1982; 48(2):521–544. [PubMed: 7119861]

Jones EG, Powell TP. Connexions of the somatic sensory cortex of the rhesus monkey. 3. Thalamic connexions. Brain. 1970; 93(1):37–56. [PubMed: 4984909]

Kaas JH, Nelson RJ, Sur M, Dykes RW, Merzenich MM. The somatotopic organization of the ventroposterior thalamus of the squirrel monkey, Saimiri sciureus. J Comp Neurol. 1984; 226(1): 111–140. [PubMed: 6736292]

Kaas JH, Qi HX, Burish MJ, Gharbawie OA, Onifer SM, Massey JM. Cortical and subcortical plasticity in the brains of humans, primates, and rats after damage to sensory afferents in the dorsal columns of the spinal cord. Exp Neurol. 2008; 209(2):407–416. [PubMed: 17692844]

Kambi N, Halder P, Rajan R, Arora V, Chand P, Arora M, Jain N. Large-scale reorganization of the somatosensory cortex following spinal cord injuries is due to brainstem plasticity. Nat Commun. 2014; 5:3602. [PubMed: 24710038]

Kaneko T, Fujiyama F. Complementary distribution of vesicular glutamate transporters in the central nervous system. Neurosci Res. 2002; 42(4):243–250. [PubMed: 11985876]

Krubitzer LA, Kaas JH. The somatosensory thalamus of monkeys: cortical connections and a redefinition of nuclei in marmosets. J Comp Neurol. 1992; 319(1):123–140. [PubMed: 1375605]

Kultas-Ilinsky K, Sivan-Loukianova E, Ilinsky IA. Reevaluation of the primary motor cortex connections with the thalamus in primates. J Comp Neurol. 2003; 457(2):133–158. [PubMed: 12541315]

Li CX, Chappell TD, Ramshur JT, Waters RS. Forelimb amputation-induced reorganization in the ventral posterior lateral nucleus (VPL) provides a substrate for large-scale cortical reorganization in rat forepaw barrel subfield (FBS). Brain Res. 2014; 1583:89–108. [PubMed: 25058605]

Li CX, Yang Q, Vemulapalli S, Waters RS. Forelimb amputation-induced reorganization in the cuneate nucleus (CN) is not reflected in large-scale reorganization in rat forepaw barrel subfield cortex (FBS). Brain Res. 2013; 1526:26–43. [PubMed: 23810455]

Liao CC, DiCarlo GE, Gharbawie OA, Qi HX, Kaas JH. Spinal cord neuron inputs to the cuneate nucleus that partially survive dorsal column lesions: A pathway that could contribute to recovery after spinal cord injury. J Comp Neurol. 2015

Liao CC, Gharbawie OA, Qi H, Kaas JH. Cortical connections to single digit representations in area 3b of somatosensory cortex in squirrel monkeys and prosimian galagos. J Comp Neurol. 2013; 521(16):3768–3790. [PubMed: 23749740]

Liao CC, Qi HX, Reed JL, Miller DJ, Kaas JH. Congenital foot deformation alters the topographic organization in the primate somatosensory system. Brain Struct Funct. 2014

Lin CS, Merzenich MM, Sur M, Kaas JH. Connections of areas 3b and 1 of the parietal somatosensory strip with the ventroposterior nucleus in the owl monkey (Aotus trivirgatus). J Comp Neurol. 1979; 185(2):355–371. [PubMed: 107204]

Manger PR, Woods TM, Munoz A, Jones EG. Hand/face border as a limiting boundary in the body representation in monkey somatosensory cortex. J Neurosci. 1997; 17(16):6338–6351. [PubMed: 9236243]

Martinez M, Brezun JM, Zennou-Azogui Y, Baril N, Xerri C. Sensorimotor training promotes functional recovery and somatosensory cortical map reactivation following cervical spinal cord injury. Eur J Neurosci. 2009; 30(12):2356–2367. [PubMed: 20092578]

Merzenich MM, Nelson RJ, Stryker MP, Cynader MS, Schoppmann A, Zook JM. Somatosensory cortical map changes following digit amputation in adult monkeys. J Comp Neurol. 1984; 224(4): 591–605. [PubMed: 6725633]

Negyessy L, Palfi E, Ashaber M, Palmer C, Jakli B, Friedman RM, Chen LM, Roe AW. Intrinsic horizontal connections process global tactile features in the primary somatosensory cortex: neuroanatomical evidence. J Comp Neurol. 2013; 521(12):2798–2817. [PubMed: 23436325]

Nelson RJ, Kaas JH. Connections of the ventroposterior nucleus of the thalamus with the body surface representations in cortical areas 3b and 1 of the cynomolgus macaque, (Macaca fascicularis). J Comp Neurol. 1981; 199(1):29–64. [PubMed: 7263946]

Pons TP, Garraghty PE, Mishkin M. Serial and parallel processing of tactual information in somatosensory cortex of rhesus monkeys. J Neurophysiol. 1992; 68(2):518–527. [PubMed: 1527572]

Pons TP, Kaas JH. Connections of area 2 of somatosensory cortex with the anterior pulvinar and subdivisions of the ventroposterior complex in macaque monkeys. J Comp Neurol. 1985; 240(1): 16–36. [PubMed: 4056103]

Pons TP, Kaas JH. Corticocortical connections of area 2 of somatosensory cortex in macaque monkeys: a correlative anatomical and electrophysiological study. J Comp Neurol. 1986; 248(3): 313–335. [PubMed: 3722460]

Qi HX, Chen LM, Kaas JH. Reorganization of somatosensory cortical areas 3b and 1 after unilateral section of dorsal columns of the spinal cord in squirrel monkeys. J Neurosci. 2011a; 31(38): 13662–13675. [PubMed: 21940457]

Qi HX, Gharbawie OA, Wong P, Kaas JH. Cell-poor septa separate representations of digits in the ventroposterior nucleus of the thalamus in monkeys and prosimian galagos. J Comp Neurol. 2011b; 519(4):738–758. [PubMed: 21246552]

Qi HX, Gharbawie OA, Wynne KW, Kaas JH. Impairment and recovery of hand use after unilateral section of the dorsal columns of the spinal cord in squirrel monkeys. Behavioural brain research. 2013; 252:363–376. [PubMed: 23747607]

Qi HX, Kaas JH. Myelin stains reveal an anatomical framework for the representation of the digits in somatosensory area 3b of macaque monkeys. J Comp Neurol. 2004; 477(2):172–187. [PubMed: 15300788]

Qi HX, Kaas JH, Reed JL. The reactivation of somatosensory cortex and behavioral recovery after sensory loss in mature primates. Front Syst Neurosci. 2014a; 8:84. [PubMed: 24860443]

Qi HX, Lyon DC, Kaas JH. Cortical and thalamic connections of the parietal ventral somatosensory area in marmoset monkeys (Callithrix jacchus). J Comp Neurol. 2002; 443(2):168–182. [PubMed: 11793354]

Qi HX, Reed JL, Gharbawie OA, Burish MJ, Kaas JH. Cortical neuron response properties are related to lesion extent and behavioral recovery after sensory loss from spinal cord injury in monkeys. J Neurosci. 2014b; 34(12):4345–4363. [PubMed: 24647955]

Ramachandran VS, Rogers-Ramachandran D, Stewart M. Perceptual correlates of massive cortical reorganization. Science. 1992; 258(5085):1159–1160. [PubMed: 1439826]

Rausell E, Bickford L, Manger PR, Woods TM, Jones EG. Extensive divergence and convergence in the thalamocortical projection to monkey somatosensory cortex. J Neurosci. 1998; 18(11):4216–4232. [PubMed: 9592100]

Shanks MF, Pearson RC, Powell TP. The ipsilateral cortico-cortical connexions between the cytoarchitectonic subdivisions of the primary somatic sensory cortex in the monkey. Brain Res. 1985; 356(1):67–88. [PubMed: 3995355]

Shi T, Apkarian AV. Morphology of thalamocortical neurons projecting to the primary somatosensory cortex and their relationship to spinothalamic terminals in the squirrel monkey. J Comp Neurol. 1995; 361(1):1–24. [PubMed: 8550872]

Stepniewska I, Gharbawie OA, Burish MJ, Kaas JH. Effects of muscimol inactivations of functional domains in motor, premotor, and posterior parietal cortex on complex movements evoked by electrical stimulation. J Neurophysiol. 2014; 111(5):1100–1119. [PubMed: 24353298]

Sur M, Nelson RJ, Kaas JH. Representations of the body surface in cortical areas 3b and 1 of squirrel monkeys: comparisons with other primates. J Comp Neurol. 1982; 211(2):177–192. [PubMed: 7174889]

Vogt BA, Pandya DN. Cortico-cortical connections of somatic sensory cortex (areas 3, 1 and 2) in the rhesus monkey. J Comp Neurol. 1978; 177(2):179–191. [PubMed: 413844]

Wall JT, Kaas JH. Long-term cortical consequences of reinnervation errors after nerve regeneration in monkeys. Brain Res. 1986; 372(2):400–404. [PubMed: 3708369]

Wong-Riley M. Changes in the visual system of monocularly sutured or enucleated cats demonstrable with cytochrome oxidase histochemistry. Brain Res. 1979; 171(1):11–28. [PubMed: 223730]

Yang PF, Qi HX, Kaas JH, Chen LM. Parallel functional reorganizations of somatosensory areas 3b and 1, and S2 following spinal cord injury in squirrel monkeys. J Neurosci. 2014; 34(28):9351–9363. [PubMed: 25009268]

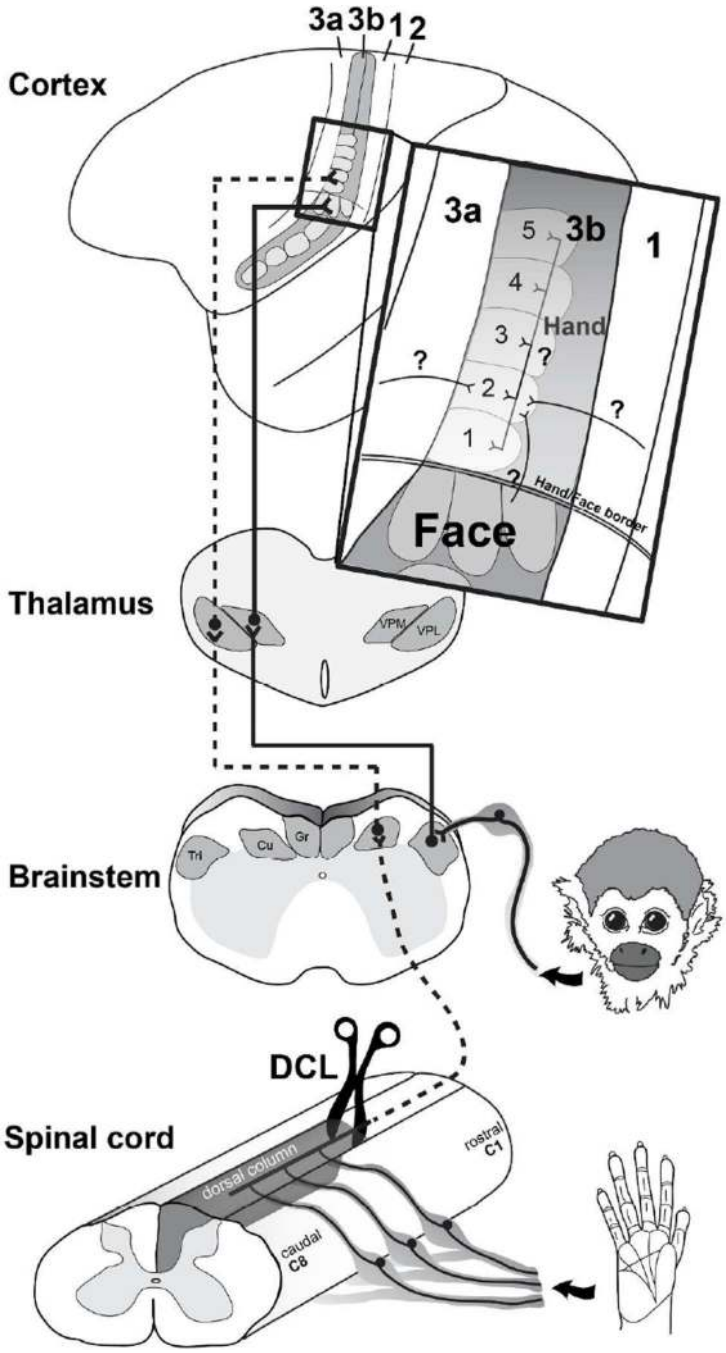

Figure 1.

A diagram showing ascending somatosensory pathways from the hand and face to the contralateral primary somatosensory area 3b. The dorsal column lesion (DCL) in the cervical spinal cord interrupts the primary inputs from the hand to the cuneate nucleus (Cu) in the brainstem, sequentially inactivating the ventroposterior lateral nucleus (VPL) in the contralateral thalamus, and the hand region of primary somatosensory area 3b. In contrast, inputs from the face remain intact and terminate on the trigeminal nucleus (Tri) in the brainstem, then ascend to the contralateral ventroposterior medial nucleus (VPM) and the

face region in area 3b. Area 3b hand neurons normally have dense intrinsic connections within area 3b and feedback projections from the hand region of other cortical areas. The representation of digit 2 in area 3b normally has stronger connections to the representations of digit 3 (black lines), and weaker connections to the representations of other digits (dark gray lines).

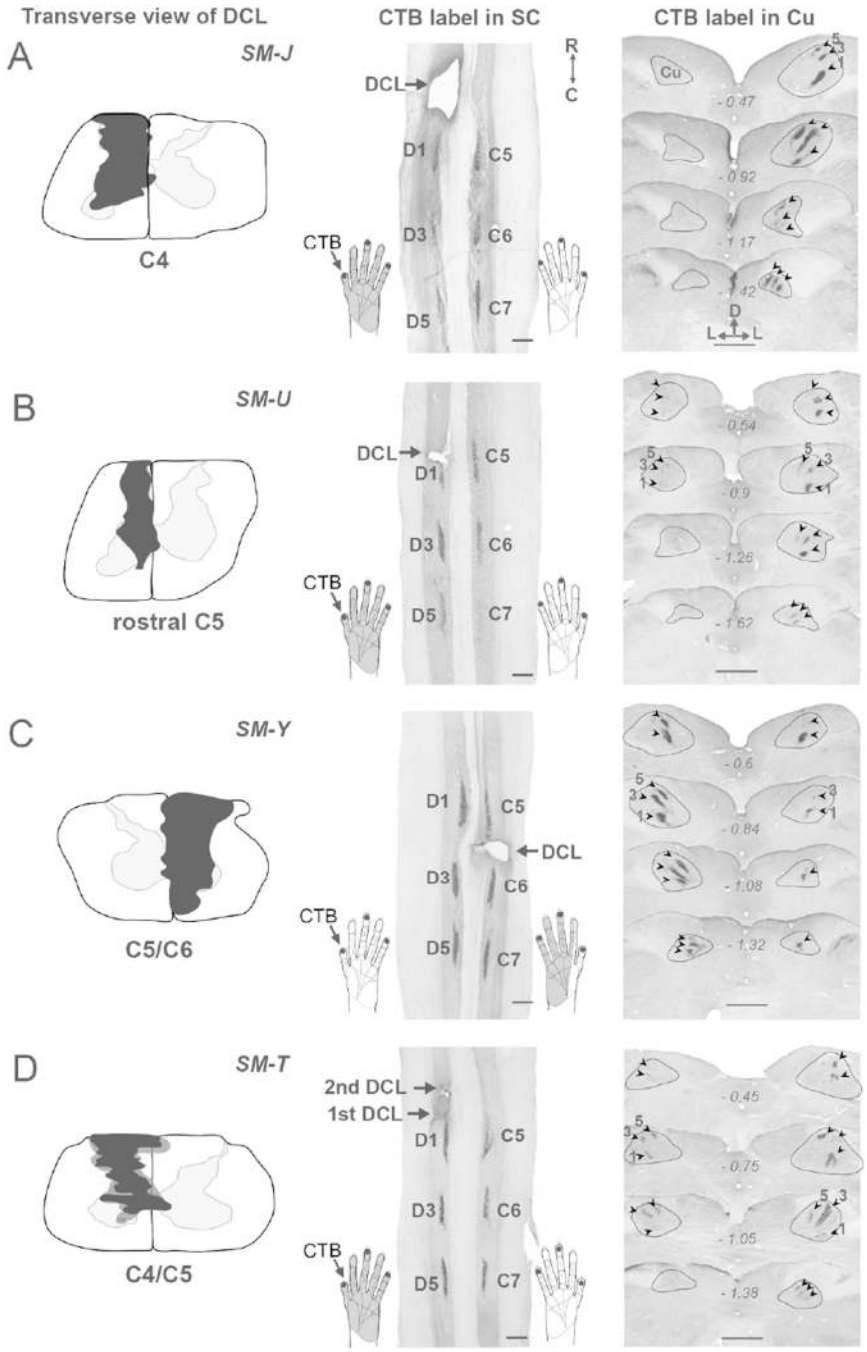

Figure 2.

Transverse view of DCLs (left column, black shading) in the spinal cord and foci of cholera toxin subunit B (CTB)-labeled terminals in the cervical spinal cord (middle column) and cuneate nuclei (right column, arrowheads) after CTB was injected into digits 1, 3, and 5 of both hands in four squirrel monkeys SM-J (**A**), SM-U (**B**), SM-Y (**C**), and SM-T (**D**). CTB injections in digits 1, 3, and 5 of both hands labeled three patches at symmetrical locations in C5, C6, and C7 of the spinal cord on both sides. In the brainstem, three foci of CTB-labeled terminals are present in the expected locations of representations of digits 1, 3, and 5

in the Cu on the intact side. The ascending projections to the Cu interrupted by DCLs resulted in different patterns of CTB-labeled foci in the Cu on the lesioned side in four monkeys. The dark gray shading in the left column of (**D**) depicts the involvement of a second DCL in monkey SM-T. The gray shading in the hand drawing in the middle column depicts the expected part of the hand that is deprived by the DCL. Numbers in the right column represent the distance in millimeters caudal to the obex. Scale bars are 1 mm.

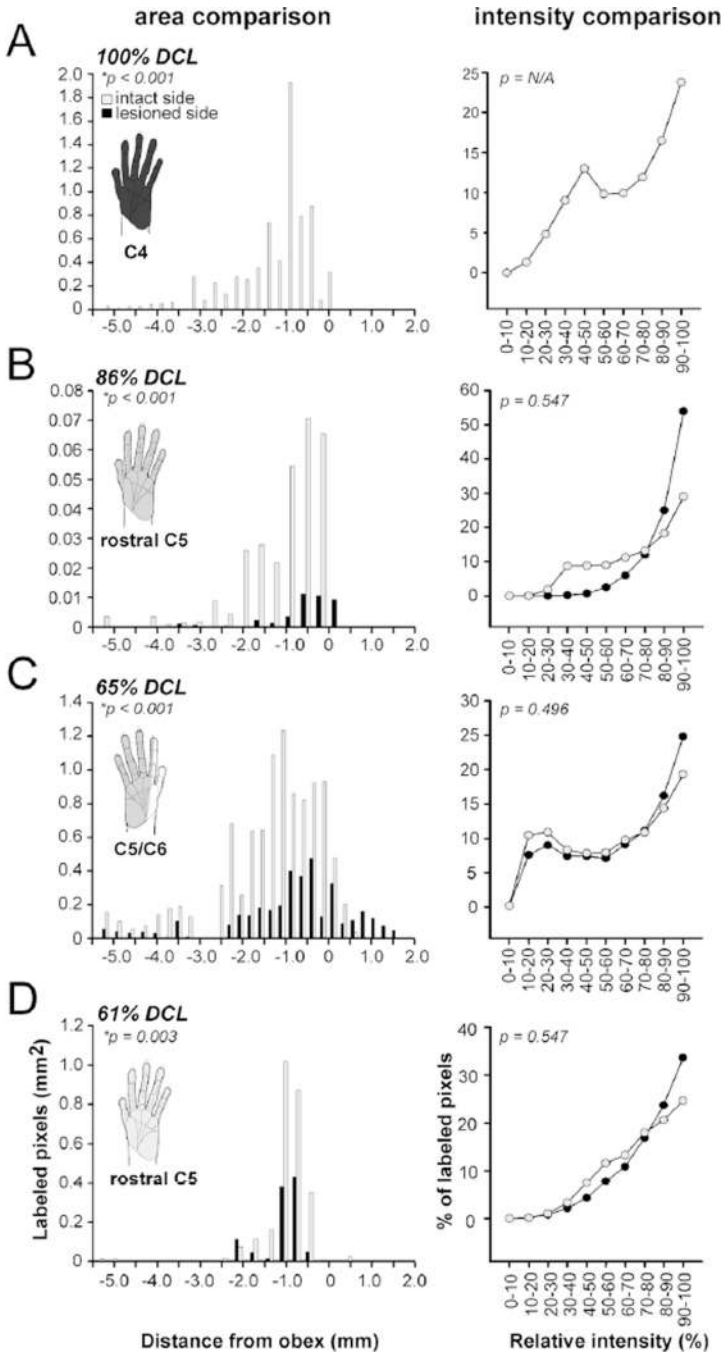

Figure 3.

Evaluation of DCL extents in four monkeys SM-J (**A**), SM-U (**B**), SM-Y (**C**), and SM-T (**D**). Left column, bar graphs showing the combined areal size of CTB-labeled foci in the cuneate nuclei on the intact (gray) and lesioned (black) sides after CTB was injected into digits 1, 3, and 5 of both hands. Numbers on the *x*–axis indicate distance of the caudal to rostral levels relative to the obex (in millimeters). The negative values indicate the measured distances caudal to the obex. The gray shading represents the affected hand region after DCLs. Differences in severity of DCL in the four monkeys are indicated by the dark to light

gray gradients. In all cases, the areas of CTB-labeled foci are significantly reduced on the lesioned side when compared to the intact side (signed-rank test, $*p < 0.05$). Right column, line diagrams showing the percentages of relative intensities of CTB-labeled pixels in the cuneate nuclei on the two sides are similar in four monkeys (signed-rank test).

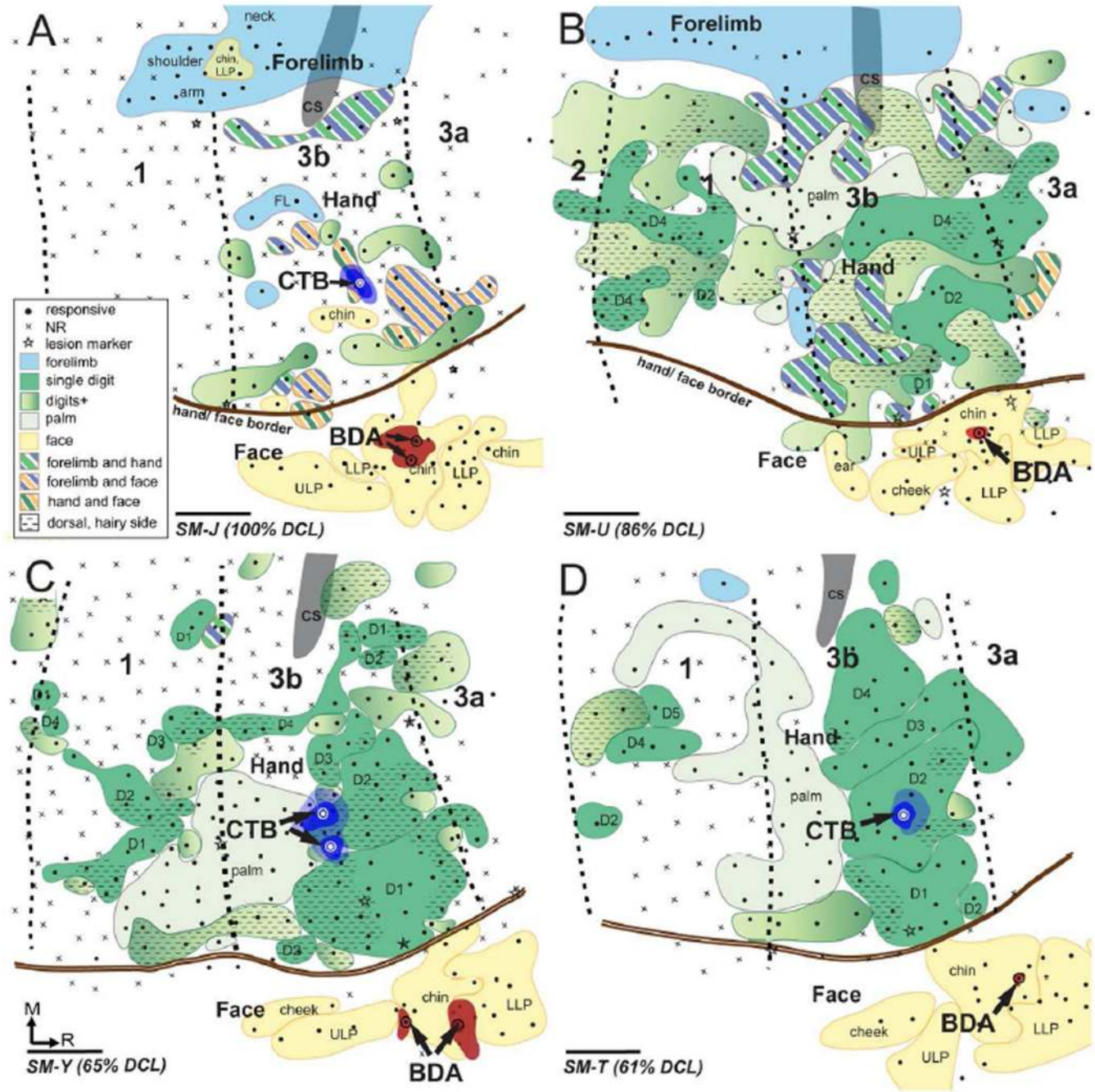

Figure 4.

Surface view of somatosensory cortex contralateral to the DCL showing topographic representations of hand and face regions in areas 3b and 1 and the locations of CTB injection sites in the hand region and BDA injection sites in the face region in area 3b in four squirrel monkeys SM-J (**A**), SM-U (**B**), SM-Y (**C**), and SM-T (**D**). Neuronal responsiveness was classified as responsive (solid circle) or no response (NR, cross). Borders separating areas 3a, 3b, and 1 were marked with electrolytic lesions (stars) during electrophysiological mapping, facilitating the estimation of areal borders (shown in this

illustration as black dashed lines). Representations of the forelimb, hand, and face are color coded in blue, green, and yellow, respectively; and representations of mixed receptive fields involving forelimb, hand, and face are shown in combinations of colored stripes accordingly. Representations of single digits are shown in solid dark green shading and representations of palm are shown in solid light green shading. The gradient of light to dark green shading depicts the representation involving multiple digits or the whole hand. CTB was injected into the expected (A) or electrophysiologically defined (B–D) representation of digit 2 in the hand region of area 3b, and BDA was injected into the representation in the face region of area 3b. Dark and light blue shadings depict cores and halos of CTB injections, respectively; and red shadings show the extents of BDA injection sites. Scale bars are 1 mm.

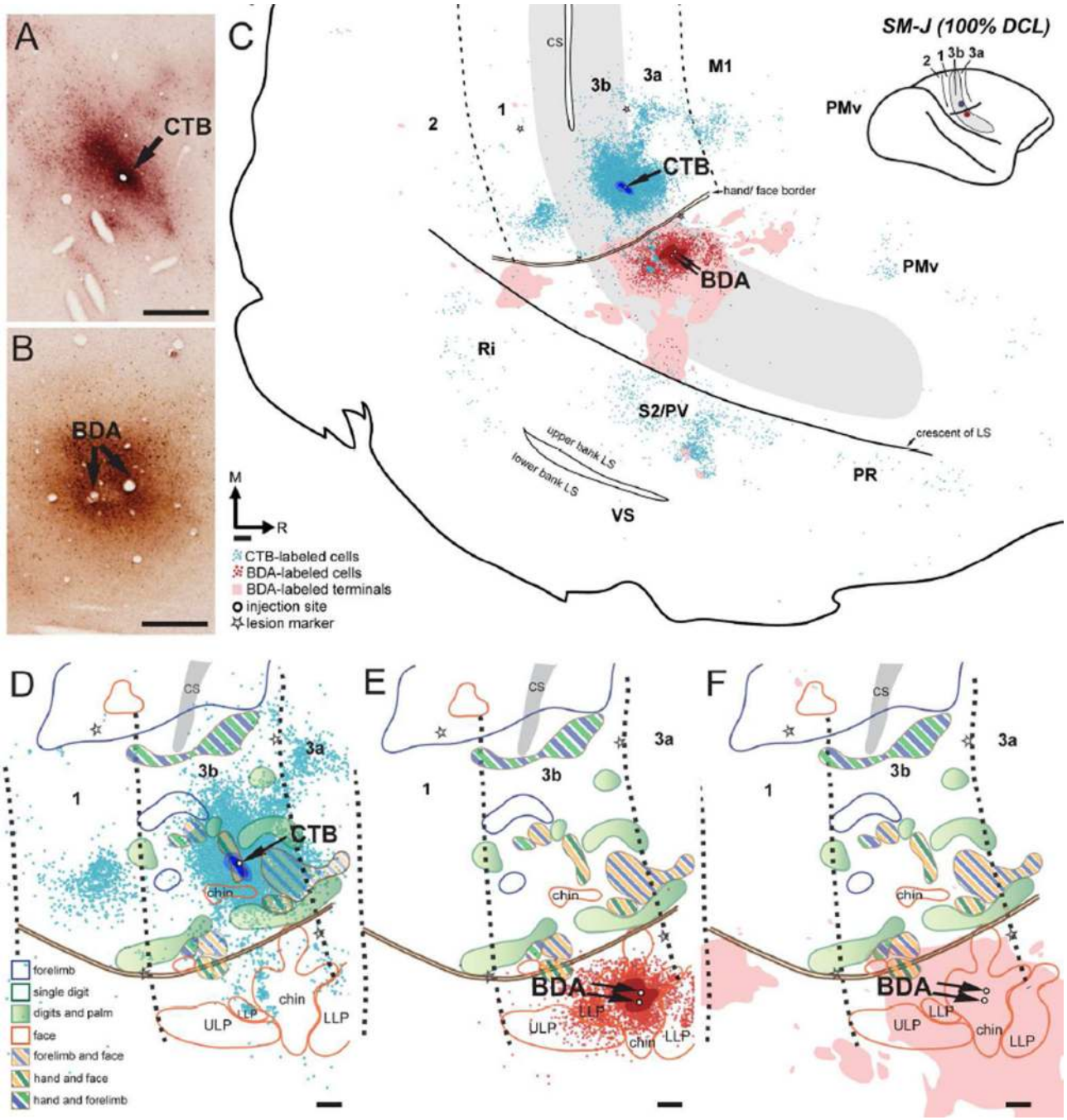

Figure 5.

Distribution of labeled neurons and terminals in the flattened cortex after CTB was injected into the hand region and BDA was injected into the face region in area 3b in monkey SM-J (100% DCL). (**A, B**) Photomicrographs showing the CTB and BDA injection sites (**C**) CTB-labeled neurons (blue dots) and BDA-labeled neurons (red dots) and terminals (pink shading) are extensively distributed in areas 3b, 1, 3a, primary motor cortex (M1), and parietal ventral (PV)/secondary somatosensory (S2) cortex. Scatterings of CTB-labeled neurons are shown in the expected locations of premotor dorsal and ventral cortex (PMd and

PMv), parietal rostral (PR), and retroinsular (Ri) cortex. Although CTB-labeled neurons are primarily confined to the hand region and BDA-labeled neurons and terminals are primarily confined to the face region in these cortical areas, a small number of CTB-labeled neurons are in the face region. CTB-labeled neurons and BDA-labeled neurons and terminals overlap in the face regions in area 3b and PV/S2. Cortical borders and the hand/face border were determined from electrolytic lesions (stars) made during electrophysiological mapping and myelinated fibers revealed in adjacent cortical sections. (**D–F**) Superimposed plots of CTB-labeled neurons, BDA-labeled neurons, and BDA-labeled terminals on the topographic representations of hand and face in areas 3b and 1 (details in Fig. 4A). Note that a small number of CTB-labeled neurons expand into the face region in area 3b (**D**). The white area in the hand region of areas 3b and 1 represents the 'No Response' zone defined by electrophysiological recordings. Scale bars are 0.5 mm.

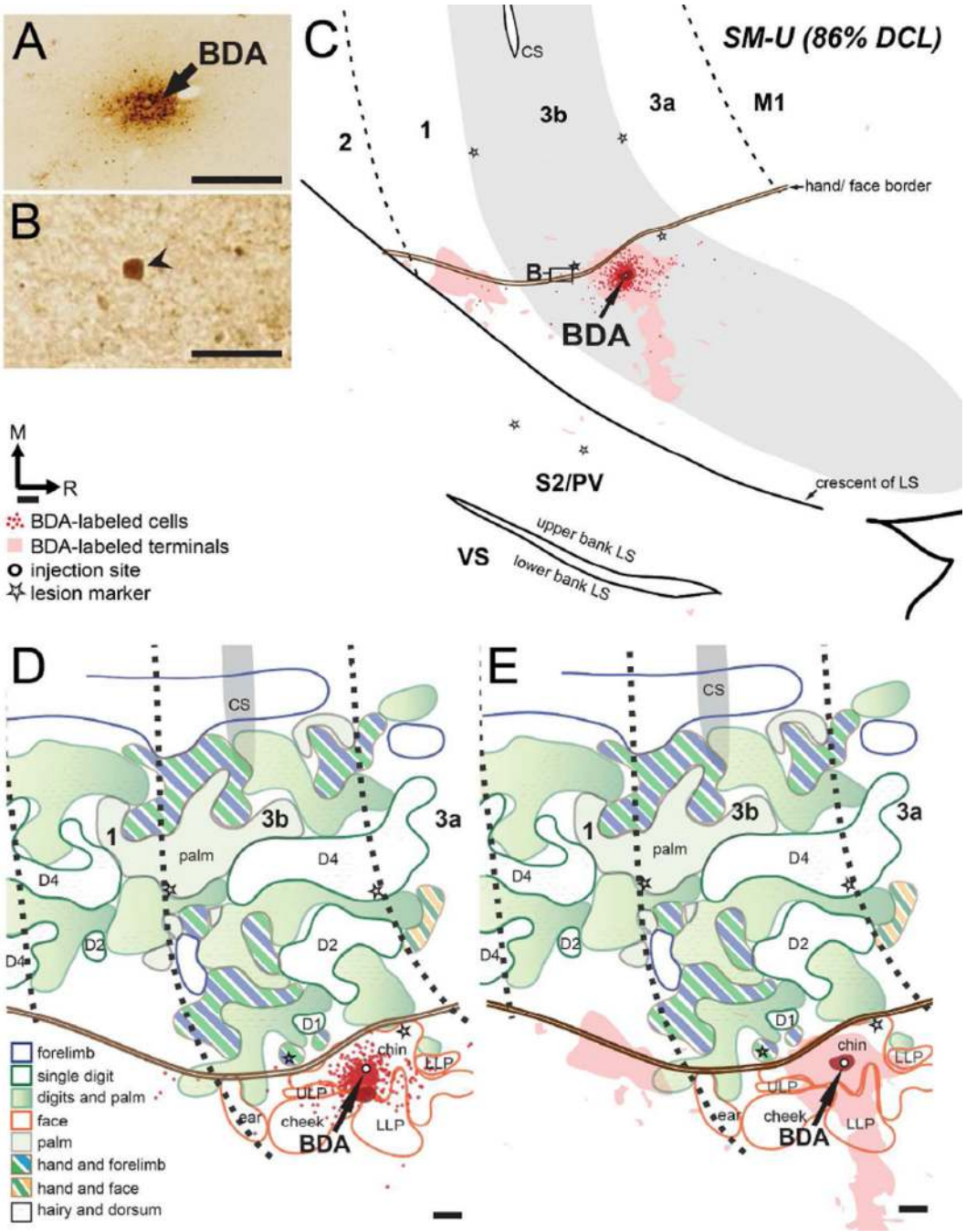

Figure 6.

Distribution of labeled neurons and terminals in the flattened cortex after BDA was injected into the face region in area 3b in monkey SM-U (86% DCL). (**A**) Photomicrographs showing the BDA injection site. (**B**) Photomicrograph showing one BDA-labeled neuron at the hand/face border of area 3b. (**C**) BDA-labeled neurons and terminals overlap in the face region of area 3b, with significantly reduced amounts in the face region of area 1. (**D, E**) Superimposed plots of BDA-labeled neurons and BDA-labeled terminals on the topographic

representations of hand and face in areas 3b and 1 (details in Fig. 4B). Scale bars are 0.5 mm in (**A, C–E**) and 300 μm in (**B**). Other conventions as in Figure 5.

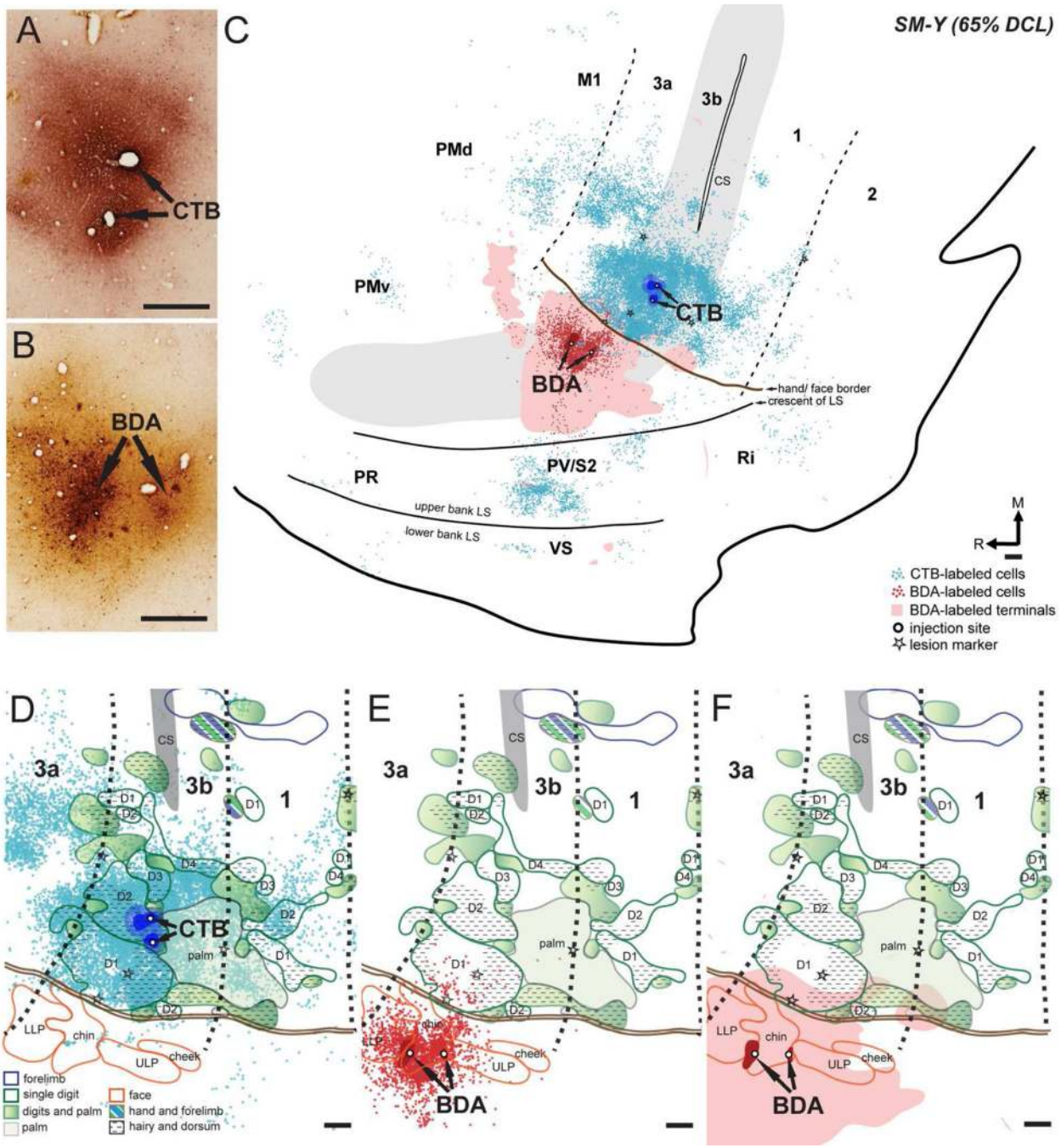

Figure 7.

Distributions of labeled neurons and terminals in the flattened cortex after CTB was injected into the hand region and BDA was injected into the face region in area 3b in monkey SM-Y (65% DCL). (**A, B**) Photomicrographs showing the CTB and BDA injection sites. (**C**) CTB-labeled neurons are extensively distributed in the hand region of areas 3b, 3a, 1, M1, and PV/S2, with small numbers in the area 2, PMd, PMv, Ri, and the ventral somatosensory cortex (VS). Note the more widespread distributions of CTB- and BDA-labeled neurons over the cortex. BDA-labeled neurons and terminals are primarily confined to the face

region in areas 3b with slight extension into the face region of area 3a and PV/S2. Overlaps of CTB-labeled neurons, BDA-labeled neurons, and BDA-labeled terminals are present in the face and hand regions in area 3b and PV/S2. (**D–F**) Superimposed plots of CTB-labeled neurons, BDA-labeled neurons, and BDA-labeled terminals on the topographic representations of hand and face in areas 3b and 1 (details in Fig. 4C). Note the small numbers of CTB-labeled neurons in the face region of areas 3b and 1 (**D**) and the slight expansion of BDA-labeled neurons (**E**) and terminals (**F**) into the hand region of area 3b. Scales are 0.5 mm in A, C–E. Other conventions as in Figure 5.

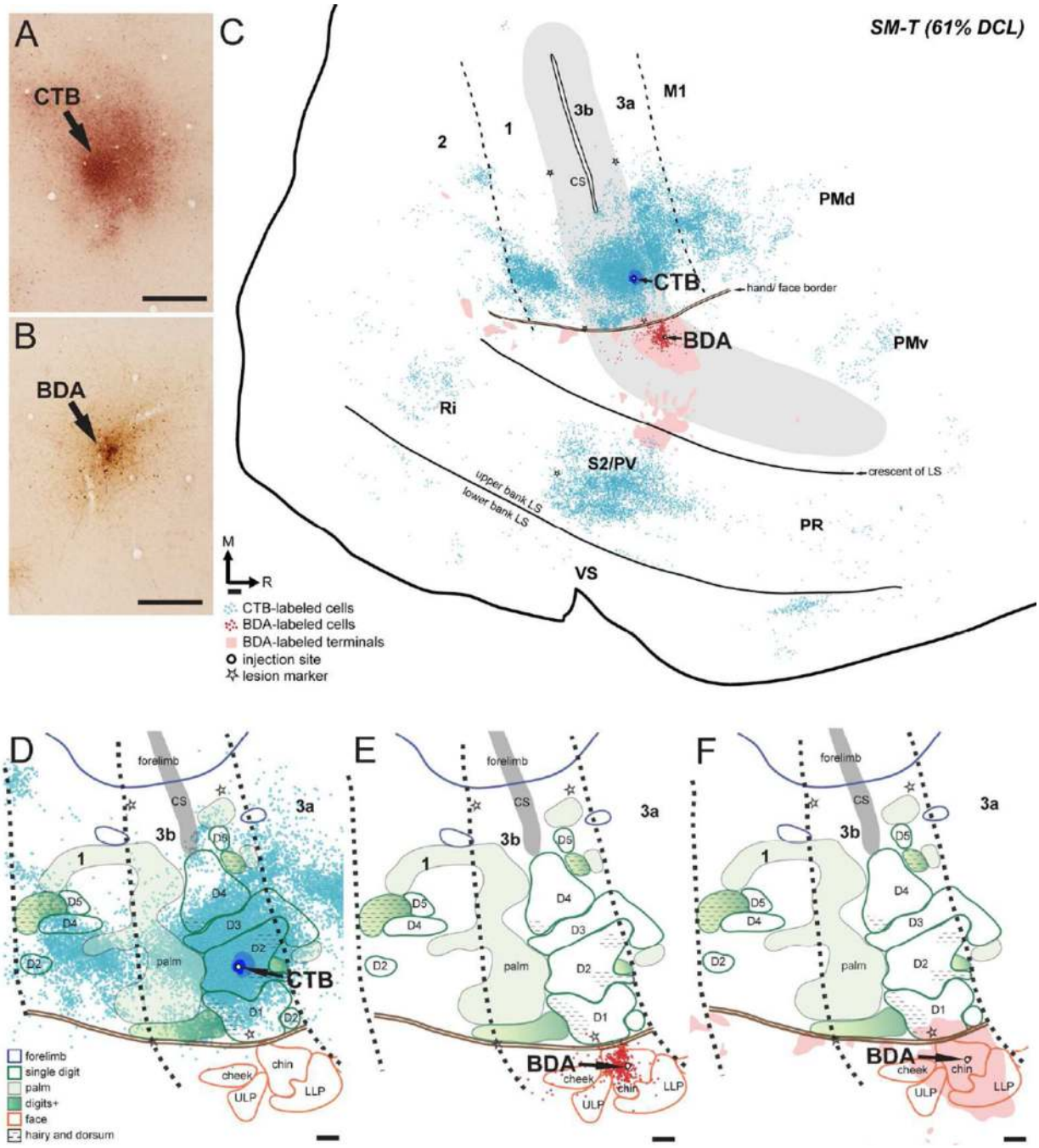

Figure 8.

Distribution of labeled neurons and terminals in the flattened cortex after CTB was injected into the hand region and BDA was injected into the face region in area 3b in monkey SM-T (61% DCL). (**A, B**) Photomicrographs showing the CTB and BDA injection sites. (**C**) CTB-labeled neurons are extensively distributed in the hand region of areas 3b, 3a, 1, M1, and S2/PV. Patches of CTB-labeled neurons are shown in PMd, PMv, Ri, and the rostral area in the cortex of the lower bank of lateral sulcus. Note the widespread distribution of CTB-labeled neurons over the cortex. BDA-labeled neurons are narrowly distributed in the face

region of area 3b, whereas the BDA-labeled terminals extend into the face region of areas 1, 2, and S2/PV. (**D–F**) Superimposed plots of CTB-labeled neurons, BDA-labeled neurons, and BDA-labeled terminals on the topographic representations of hand and face in areas 3b and 1 (details in Fig. 4D). Scales are 0.5 mm in A, C–E. Other conventions as in Figure 5.

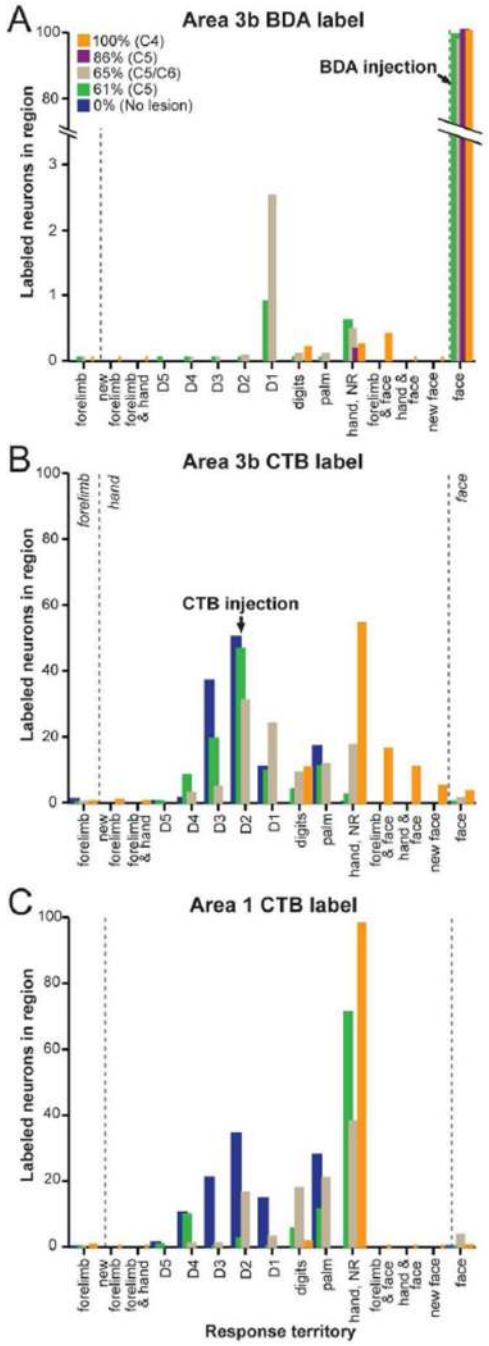

Figure 9.

Distribution of percentages of CTB- and BDA-labeled neurons in relation to altered somatotopic representations in areas 3b (**A, B**) and 1 (**C**). Injection into the face region (**A**) was made in the representation of chin in area 3b, and injections into the hand region (**B, C**) were made in the expected territory of digit 2 in the hand region in all cases. Dashed lines indicating the expected territory of the forelimb, hand, and face regions are shown in background. Data from CTB injections in the hand region in two normal monkeys (0%; blue) described in our previous publication (Liao et al., 2013) used for comparison reveal

the differences in the distributions of the percent of labeled neurons after DCLs. Data from the four DCL monkeys that had various lesion extents (%) and levels are shown in different colors. The percentages of labeled neurons in somatotopic representations in area 3b from all cases were obtained from superimposing the plots of labeled neurons on the electrophysiologically defined maps. However, in normal monkeys, the borders of the digit representations in area 1 were not fully defined electrophysiologically. Thus, the percentages of labeled neurons in the hand region in area 1 in normal monkeys were obtained from superimposing the plots on the estimated borders of digits representations (**9C**). For visualization purpose, the highest value from one normal monkey is shown.

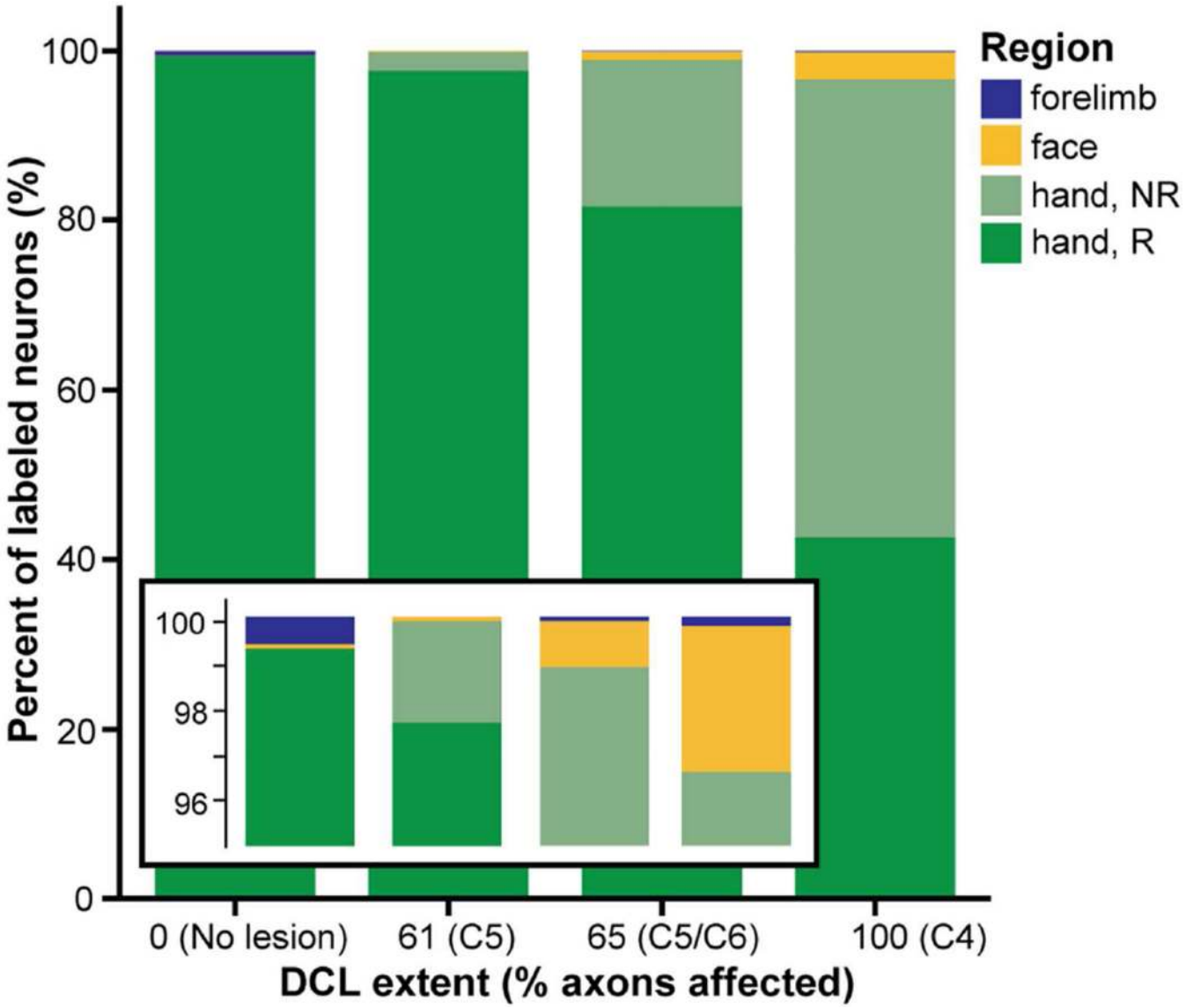

Figure 10.

Proportion of area 3b neurons labeled by CTB injections into the hand region of area 3b in three (of four) cases with different extents and levels of DCL. Data from two monkeys with no lesions (0%) described in our previous publication (Liao et al., 2013) were included to show normal proportions (by weighted average of the neuron counts) and possible alterations after DCLs. Stacked bars show the proportions of labeled neurons by somatotopic region to sum to 100% of the labeled neurons in each category of lesion extent from 0 (no lesion) to 100 (complete lesion). Regions of hand, face, and forelimb estimated by anatomical landmarks and somatotopic mapping are indicated in green, yellow, and blue, respectively. The percentage of labeled neurons found in the territory of the hand that did not respond to tactile stimulation on hand, face, and forelimb is indicated in light green (Hand, NR). Each region is represented within each lesion category; however, the proportions of labeled neurons in some of the body representations are very small (particularly the forelimb region, 0–0.6%, see the enlarged view in inset). Overall, the

percentage of labeled neurons in the hand region was similarly high across all cases. The more extensive DCLs resulted in greater proportions of labeled neurons overlapping the cortex in the hand region that was unresponsive to stimulation, as well as greater proportions of labeled neurons in the face regions.

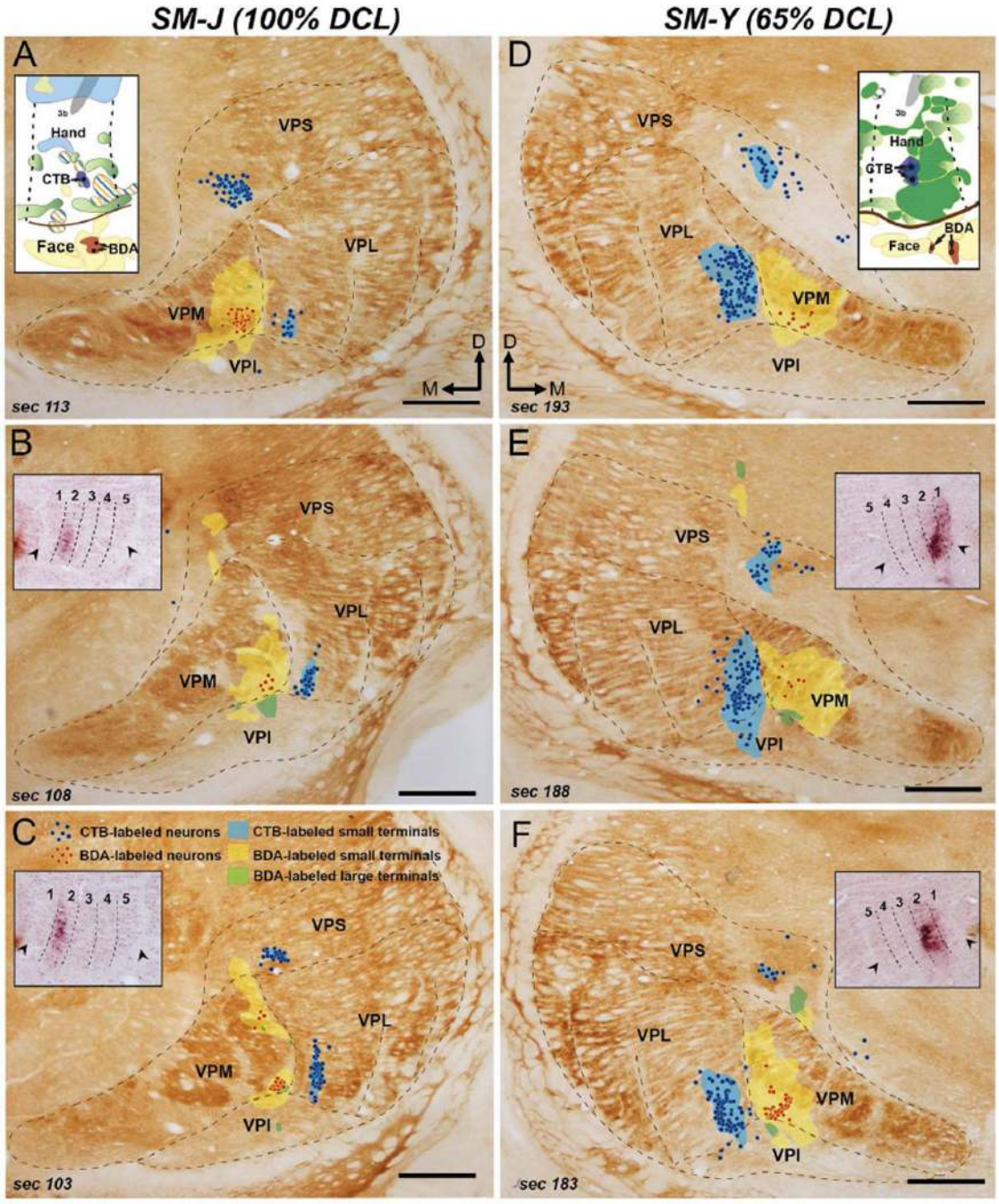

Figure 11.

Distribution of CTB- and BDA-labeled neurons and terminals in the thalamus after CTB was injected into the hand region of area 3b and BDA was injected into the face region of area 3b in monkeys SM-J (**A–C**) and SM-Y (**D–F**). Plots of label are superimposed on the adjacent CO sections that reveal the structural architecture in the thalamus. Insets in (**A**) and (**D**) show tracer injection sites in area 3b (details in Fig. 4A, C). Insets in (**B**), (**C**), (**E**), and (**F**) show photomicrographs of the CTB-labeled neurons and terminals in the ventroposterior lateral nucleus (VPL); arrowheads mark the medial-lateral extent of the hand representation

in VPL, and dashed lines indicate septa that separate the representations of digits 1–5 revealed by CO staining. Note that CTB-labeled neurons (blue circles) and terminals (blue shading) are restricted to the territory of VPL, and BDA-labeled neurons (red circles) and terminals (yellow shading: small size; green shading: large size) are restricted to the territory of ventroposterior medial nucleus (VPM). Small numbers of CTB-labeled neurons and BDA-labeled terminals are distributed in the ventroposterior inferior (VPI) and ventroposterior superior (VPS) nucleus. Scale bars are 1 mm.

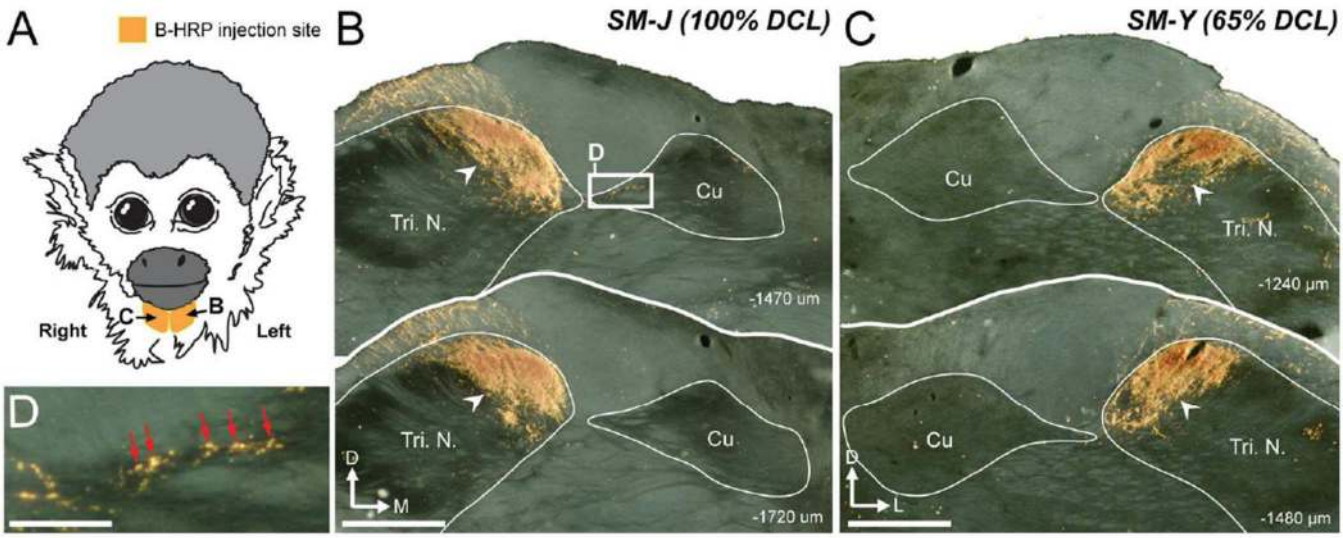

Figure 12.

Distribution of labeled terminals in the brainstem after cholera toxin subunit B conjugated with wheat germ agglutinin-horseradish peroxidase (B-HRP) was injected into the anterior chin ipsilateral to the DCL. (**A**) B-HRP injection sites. (**B**) In monkey SM-J (100% DCL), B-HRP-labeled terminals were primarily distributed in the trigeminal nucleus (Tri, white arrowheads) but slightly intruded into the cuneate nucleus (Cu; inset D). (**C**) In monkey SM-Y (65% DCL), B-HRP-labeled terminals were restricted to the Tri. No B-HRP labeled terminals were found in the Cu. (**D**) Photomicrograph showing the B-HRP labeled terminals in the Cu. Scale bars are 1 mm in B, C and 100 µm in D.

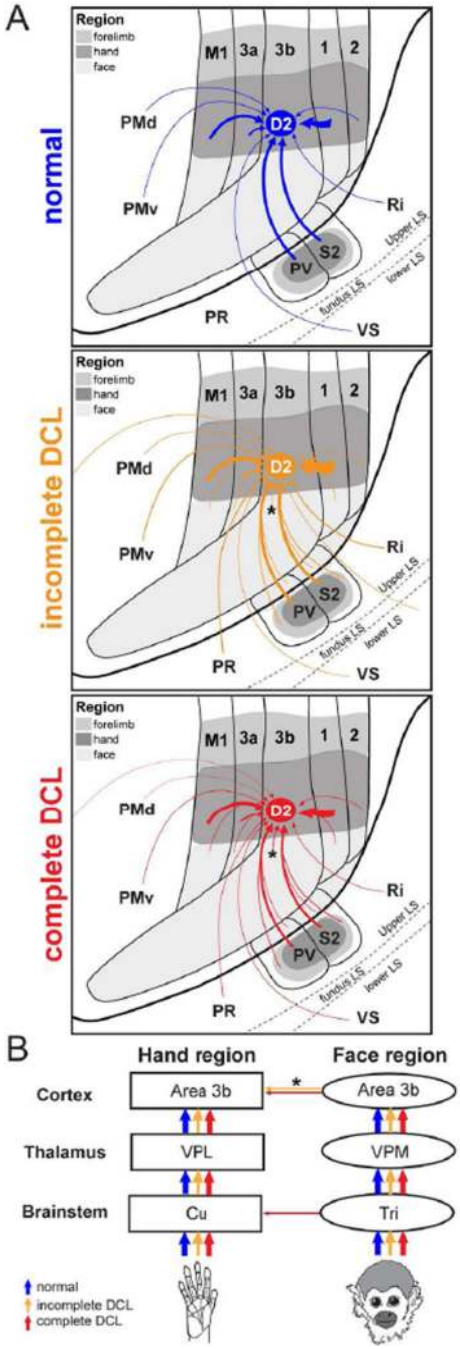

Figure 13.

Summary diagrams depicting how the extent of DCL in the cervical spinal cord altered the intracortical connections of the hand region (expected location of digit 2 representation) in area 3b (**A**) and the anatomical connections of the hand and face regions in brainstem, thalamus, and cortex (**B**). Territories of the hand, forelimb, and face regions are shown in dark to light gray, respectively. The thickness of each line represents the relative density of the connection. Results from normal, incomplete DCL, and complete DCL monkeys are in shown blue, orange, and red, respectively. Note, in addition to the pre-existing connections

from the hand region of areas 3a, 1, 2, and PV/S2 and other cortical areas in normal monkeys; after long-term DCL, the hand region in area 3b is additionally connected to the face region in area 3b (asterisks in **A** and **B**) and areas 3a, 1, 2, and PV/S2.

Table 1

Abbreviations

3a, Area 3a
3b, Area 3b
1, Area 1
2, Area 2
D1– 5, Digits 1 – 5
BDA, Biotinylated dextran amine
B-HRP, Cholera toxin subunit B conjugated with wheat germ agglutinin-horseradish peroxidase
C, Caudal
C1 – C8, Spinal cord cervical segments 1 – 8
CO, Cytochrome oxidase
CS, Central sulcus
CTB, Cholera toxin subunit B
Cu, Cuneate nucleus of brainstem
D, Dorsal
D1 – D5, Digits 1 – 5
DAB, 3,3-diaminobenzidine tetrahydrochloride
DCL, Dorsal column lesion
F, Myelinated fibers
L, Lateral
LLP, Lower lip
LS, Lateral sulcus
M, Medial
M1, Primary motor area
NR, No response
PMd, Dorsal premotor area
PMv, Ventral premotor area
PR, Parietal rostral somatosensory area
PV, Parietal ventral area
R, Rostral
RF, Receptive field
Ri, Retroinsular cortex
S2, Second somatosensory area
TMB, 3,3,5,5-tetramethylbenzidine
Tri, Trigeminal nucleus of brainstem
ULP, Upper lip
VGLUT2, Vesicular glutamate transporter 2
VP, Ventroposterior nucleus of thalamus
VPI, Ventroposterior inferior nucleus of thalamus
VPL, Ventroposterior lateral nucleus of thalamus
VPM, Ventroposterior medial nucleus of thalamus

VPS, Ventroposterior superior nucleus of thalamus

VS, Ventral somatosensory area

WGA-HRP, Wheat-germ agglutinin conjugated with horseradish peroxidase

Table 2

Table of Primary Antibody Used

Primary antibody antigen	Immunogen	Source; host species; cat#; RRID	Concentration
vesicular glutamate transporter 2 (VGLUT2)	Full length of recombinant protein from rat VGLUT2	Millipore, Billerica, MA; mouse monoclonal; MAB5504; AB_2187552	1:5000

Table 3

Percent of BDA-labeled neurons after injections in area 3b face region with estimated pairwise differences by lesion extents

Response territory	Compare DCL (A–B)	Contrast estimate	Percent (A)	Percent (B)	Significance (adjusted)
Face	61% – 65%	1.65	98.6	96.9	< 0.0001
	61% – 86%	−1.28	98.6	99.9	< 0.0001
	61% – 100%	−0.89	98.6	99.5	< 0.0001
	65% – 86%	−2.92	96.9	99.9	< 0.0001
	65% – 100%	−2.54	96.9	99.5	< 0.0001
	86% – 100%	0.39	99.9	99.5	< 0.0001
Hand	61% – 65%	−0.32	0.12	0.44	1.000
	61% – 100%	−0.04	0.12	0.16	1.000
	65% – 100%	0.27	0.44	0.16	1.000
Hand, No response	61% – 65%	0.14	0.56	0.43	< 0.0001
	61% – 86%	0.43	0.56	0.14	< 0.0001
	61% – 100%	0.37	0.56	0.20	< 0.0001
	65% – 86%	0.29	0.43	0.14	< 0.0001
	65% – 100%	−0.23	0.43	0.20	< 0.0001
	86% – 100%	−0.06	0.14	0.20	< 0.0001
Forelimb & face	100%		0.36		

Table 4

Percent of CTB-labeled neurons after injections in area 3b hand region with estimated pairwise differences by lesion extents

Response territory	Compare DCL (A–B)	Contrast estimate	Percent (A)	Percent (B)	Significance (adjusted)
Forelimb	61% – 0%	−0.36	0.02	0.38	0.65
	61% – 65%	−0.06	0.02	0.08	< 0.0001
	61% – 100%	−0.13	0.02	0.16	< 0.0001
	65% – 0%	−0.30	0.08	0.38	0.65
	65% – 100%	−0.07	0.08	0.16	< 0.0001
	100% – 0%	−0.22	0.15	0.38	0.65
Hand, No Response	61% – 65%	−15.0	2.24	17.3	< 0.0001
	61% – 100%	−51.8	2.24	54.0	< 0.0001
	65% – 100%	−36.8	17.3	54.0	< 0.0001
Hand Response	61% – 0%	−2.65	12.5	14.2	1.000
	61% – 65%	0.35	12.5	14.1	1.000
	61% – 100%	3.30	12.5	13.8	1.000
	65% – 0%	−2.99	14.1	14.2	1.000
	65% – 100%	2.96	14.1	13.8	1.000
	100% – 0%	−5.95	13.8	14.2	1.000
Face	61% – 0%	0.05	0.10	0.05	< 0.0001
	61% – 65%	−0.92	0.10	1.02	< 0.0001
	61% – 100%	−3.06	0.10	3.16	< 0.0001
	65% – 0%	0.98	1.02	0.05	< 0.0001
	65% – 100%	−2.14	1.02	3.16	< 0.0001
	100% – 0%	3.12	3.16	0.05	< 0.0001

Continued for subdivisions of response territories not analyzed statistically

Hand & arm	100%		0.25		
Hand & face	100%		10.6		

Response territory	Compare DCL (A–B)	Contrast estimate	Percent (A)	Percent (B)	Significance (adjusted)
New face	100%		4.85		
D5	61% – 0%	0.000	0.15	0.15	
D4	61% – 0%	7.34	8.08	0.74	
	61% – 65%	5.48	8.08	2.59	
	65% – 0%	1.85	2.59	0.74	
D3	61% – 0%	−10.03	19.16	29.20	
	61% – 65%	14.51	19.16	4.65	
	65% – 0%	−24.54	4.65	29.20	
Continued for subdivisions of response territories not analyzed statistically					
D2	61% – 0%	−0.61	46.4	46.96	
	61% – 65%	15.7	46.4	30.68	
	65% – 0%	−16.3	30.7	46.96	
D1	61% – 0%	−0.97	9.3	10.3	
	61% – 65%	−14.3	9.3	23.6	
	65% – 0%	13.3	23.6	10.3	
Digits	61% – 65%	−4.99	3.78	8.78	
Palm	61% – 0%	−1.44	10.8	12.2	
	61% – 65%	−0.54	10.8	11.3	
	61% – 100%	0.13	10.8	10.7	
	65% – 0%	−0.91	11.3	12.2	
	65% – 100%	0.66	11.3	10.7	
	100% – 0%	−1.57	10.6	12.2	

D1-D5, digits 1–5.